Response to Reviewer #1:

The authors of the present manuscript acknowledge the reviewer for carefully reading and providing constructive comments that have led to an improved paper. Responses are written in blue text.

1. Page 6, Line 23, "700 hPa and LTS is. . .. . ." should be "700 hPa and LTS are.....".

Response: Done.

2. Page 7, Line 13, "Figure 2 shows....." should be "Figure 2 shows. . .. . .".

Response: Done.

3. What's the meaning of "P" in Figure 6?

Response: P is the statistical probability. This information has been added to Figure 6's caption.

4. Page 8, Line 4-5, "This indicates that strong surface wind speeds transported smaller aerosol particles with no optical sensitivity from the continental interior to over the site", how to get the conclusion that the smaller aerosols are transported from the continental interior?

Response: We found that this statement is not fully supported by the current dataset and analysis. We have thus removed the sentences "However, relatively large aerosol number concentrations were measured. This indicates that strong surface wind speeds transported smaller aerosol particles with no optical sensitivity from the continental interior to over the site." from the revised manuscript.

5. Why do the periods shown in red box in Figure 5 represent the periods of new particle formation and growth?

Response: From an observational point of view, atmospheric new particle formation and subsequent particle growth are seen as the emergence of new aerosol particles into the lower end of the measured particle size spectrum (e.g., particle sizes below 50 nm), followed by the growth of these particles into larger sizes (Kulmala et al., 2012). The periods outlined in red show that aerosol particles start off small then grow larger.

[Kulmala, M., et al., 2012. Measurement of the nucleation of atmospheric aerosol particles. Nat. Protoc. 7, 1651–1667.]

6. Page 9, Line 15. Actually, as shown in Nakajima et al (2001) and Liu and Li (2014), aerosol index is defined as the product of AOD and AE. However, in this study, aerosol index is defined as the product of the surface-measured aerosol scattering coefficients and AE in this study?

Response: We have changed the term "aerosol index" to "scattering aerosol index", which has been used in related studies (e.g., Liu and Li, 2014; Sena et al., 2016). We have also deleted the reference to Nakajima et al. (2001) because they define the scattering aerosol index differently.

[Liu, J., and Li, Z.: Estimation of cloud condensation nuclei concentration from aerosol optical quantities: influential factors and uncertainties, Atmos. Chem. Phys., 14(1), 471–483, https://doi.org/10.5194/acp-14-471-2014, 2014.

Sena, E. T., McComiskey, A., and Feingold, G.: A long-term study of aerosol-cloud interactions and their radiative effect at the Southern Great Plains using ground-based measurements, Atmos. Chem. Phys., 16, 11,301–11,318, doi:10.5194/acp-16- 11301-2016, 2016.]

7. The linear regression slopes need be given in Figure 7.

Response: The slopes have now been given in Figures 7 and 8.

8. Page 10, Line 30, "Figure 8c and 8d suggests ..." should be "Figure 8c and 8d suggest ..."

Response: Done.

9. Page 11, Line 6, "Figures 8 ..." should be "Figure 8 ..."

Response: Done.

10. Page 11, Line 10, "... suggests that ..." should be "... suggest that ..."

Response: Done.

11. What is the lack of samples for cluster II air-mass condition? Why cannot use the cluster II to calculate FIE?

Response: As shown in Figure 10, combined cloud and aerosol data need to be separated into narrow LWP bins to calculate the FIE. There were not enough cloud and aerosol samples in each narrow LWP bin for the cluster II air mass to avoid large uncertainties in the FIE estimates. Furthermore, only cases with sample numbers greater than 50 and with calculated values of FIE that are statistically significant at the 95% confidence level (P = 0.05) are discussed in the study. To make things clearer, we have changed the sentence "Due to the lack of samples …" to "Since there were not enough samples under cluster II air-mass condition …". We also added the sentence "Only those cases with sample numbers greater than 50 per bin and where the calculated values of FIE are statistically significant at the 95% confidence level (P = 0.05) are analyzed here." to the revised manuscript.

12. Page 13, Line 6, "... can is possibly because ..." should be "... can be possibly because ..."

Response: Done.

13. Page 14, Line 12-15, "... more inorganic compounds that when ..." should be "... more inorganic compounds than that when ..."

Response: Sentence corrected.

Response to Reviewer #2

The authors of the present manuscript acknowledge the reviewer for carefully reading and providing constructive comments that have led to an improved paper. Responses are written in blue text.

Page 1. Line 26-29, please modify the sentence to correct the grammar.

Response: The sentence has been changed to "Under low aerosol loading conditions, the liquid water path (LWP) and droplet effective radius (DER) significantly increased with increasing LTS, but under high aerosol loading conditions, LWP and DER changed little, indicating that aerosols significantly weakened the dependence of cloud development on LTS."

Page 1, Line 30, either "a stable condition" or "stable conditions"

Response: Fixed.

Page 2. line 2, you may remove "with increasing LWP"

Response: We have removed "with increasing LWP".

Page 2, Line 3-5, grammar error for "can significantly made", also "narrowed"

Response: The sentence has been changed to "Under both continental and marine air-mass conditions, high aerosol loading can significantly shift COD towards larger values and LWP and DER towards smaller values, narrowing the distributions of LWP and DER."

Page 2, Line 15-28, many references should be cited here. For example, the aerosol direct effect (Yang et al. 2016, 2018; doi:10.1002/2016JD024938, doi: 10.1016/j.atmosres.2018.04.029), the aerosol indirect effect (Feingold et al., 2003; Garrett et al., 2004; Zhao et al., 2018, 2019), lifetime effect (Albrecht 1989), thermal emissivity effect (Zhao and Garrett, 2006; Garrett and Zhao, 2015); semi- direct effect (Koren et al.). Feingold, et al., First measurements of the Twomey indi- rect effect using ground-based remote sensors, Geophys. Res. Lett., 30(6), 1287, doi:10.1029/2002GL016633, 2003. Garrett, et al., 2004: Effects of varying aerosol regimes on low-level Arctic stratus. Geophys. Res. Lett., 31, L17105. Zhao, et al. (2018). Negative Aerosol-Cloud re Relationship from Aircraft Observations over Hebei, China. Earth and Space Science, 5, 19-29. Zhao, et al. (2019), A case study of stratus cloud properties using in situ aircraft observations over Huanghua, China, Atmosphere, 10, 19. Albrecht, B.A., 1989: Aerosols, cloud microphysics, and fractional cloudiness, Science, 245(4923), 1227-1230. Garrett, T. J. and C. Zhao, 2006: In- creased Arctic cloud longwave emissivity associated with pollution from mid-latitudes. Nature, 440, nature04636, 787-789. Zhao, C., and T. Garrett, 2015: Effects of Arctic haze on surface cloud radiative forcing, Geophys. Res. Lett., 42, 557-564, doi:10.1002/2014GL062015.

Response: The suggested references have been added to the revised manuscript.

Page 2, Line 32, for surface remote sensing, Garrett et al. (2004) and Qiu et al. (2017, 8-Year ground-based observational analysis about the seasonal variation of the aerosol-cloud droplet effective radius relationship at SGP site) should be cited.

Response: They have now been cited.

Page 3, Line 2, for aircraft measurement-based studies, Yang et al. (2019, Toward understanding the process-level impacts of aerosols on microphysical properties of shallow cumulus cloud using aircraft observations) and Zhao et al. (2018, 2019) should be cited, which are for North China region.

Response: They have now been cited.

Page 3. Line 17-20, The effect is also dependent on the availability of water vapor, or the amount of water vapor, and meteorology (such as vertical velocity), as indicated by Qiu et al. (2017) and Yang et al. (2019).

Response: Yes, we agree. The suggested references have now been cited.

Page 3, Line 22-23, Garrett et al. (2004) also examined the sensitivity of FIE to aerosol size and number, which shows weak sensitivity of FIE to aerosol number concentration for those small sizes, but good sensitivity for aerosols with relatively large size (such as CCN or accumulation mode aerosol).

Response: We added the sentence "Garrett et al. (2004) indicated a weak sensitivity of FIE to aerosols with small particle sizes but a stronger sensitivity to aerosols with relatively large sizes." to the revised manuscript.

Page 4. Line 13-14, What is the maximum size for Na? You might also give this information.

Response: We have added this information and changed the sentence to "with diameters larger than 10 nm and smaller than 3 μm".

Page 5 Line 10-21, The uncertainty information for cloud boundaries should be provided. As indicated by Zhao et al. (2012, Toward Understanding of Differences in Current Cloud Retrievals of ARM Ground-based Measurements) and Zhao et al. (2013, Ground-based remote sensing of thin clouds in the Arctic), the uncertainties in cloud bases and tops measured by ARM are generally 7.5 m and 45 m, respectively.

Response: We have added the sentence "The cloud-base and cloud-top height uncertainties are ~7.5 m and ~45 m, respectively (Zhao et al., 2012a; Garrett and Zhao, 2013)." to the revised manuscript.

Page 5. Line 28, "density of liquid water", and COD is cloud optical depth at visible wavelength.

Response: Done.

Page 8, Line 12-15, please check and correct the grammar here.

Response: The sentence has been changed to "When the continental air-mass influenced the site, fine particles dominated aerosol scattering and were responsible for ~65% of the total particle scattering, indicating that more anthropogenic aerosols with small particle sizes were transported to the site from continental regions to the west."

Page 10, Line 1-5, Other studies as mentioned earlier have also indicated this likely evaporation and entrainment effect near cloud tops, which could be cited.

Response: Done.

Page 10, Line 7, “can possible” -> “can be possible”

Response: The sentence has been changed to “The changes in DER with LTS possibly reflect the changes in LWP with LTS due to the high positive correlation between LWP and DER (Zhang et al., 2011; Sporre et al., 2014).”

Page 10, Line 10-14, Yang et al. (2019), Zhao et al. (2018, 2019) have also made similar descriptions.

Response: These references are now cited.

Page 12, Line 20-21, Zhao et al. (2012) have indicated that using different aerosol variables to represent the aerosol loading amount, the quantified FIE values could vary, which is worthy to be mentioned here.

Response: It has already been mentioned in section 3.3.2.

Page 13, Line 11, also Zhao et al. (2012); Lin 12-13, Yang et al. (2019) too.

Response: These references are now cited.

Page 13, Line 24, I would suggest “the question how sensitive the cloud properties are sensitive to ...”

Response: The sentence has been changed to “Examined next is the sensitivity of cloud properties to aerosol chemical composition represented by the mass fraction of organics.”

Page 13, Line 26, what is the size range for the aerosol concentration?

Response: The size range for the aerosol concentration is 10 nm to 3 μm in diameter. This is mentioned in section 2.1.1.

Page 14, Line 13, “larger”?

Response: Done.

Response to Reviewer #3

The authors of the present manuscript acknowledge the reviewers for carefully reading and providing constructive comments that have led to an improved paper. Responses are written in blue text.

1. Page 4, Line 23. What is the temporal resolution of Na and aerosol optical properties used in this study?

Response: The temporal resolution is one minute. This information has been added to section 2.1.1: "The time resolution of the N_a, σ_s, and σ_a measurements is one minute."

2. Page 6, Line 25. LTS is calculated at 1-min resolution?

Response: The temporal resolution is one hour. This information has been added to section 2.3: "The European Centre for Medium-Range Weather Forecasts model runs for ARM analysis with a one-hour resolution for a 0.56^o x 0.56^o box centered on the site provided values of ω and potential temperature."

3. Page 6, Line 29. Please specify how to collocate the datasets of different time resolutions (e.g. ACSM, AOS, LTS, large-scale vertical velocity and cloud properties) for the comparisons later on in the manuscript, particularly shown in Figure 10 & 11. And the final temporal resolution for collocated data.

Response: Most of the datasets, i.e., aerosol properties (scattering coefficients and number concentrations) from the AOS, cloud properties (COD, LWP, DER), and surface meteorology, have a 1-min temporal resolution. These data were first matched according to the observation time, and then matched with aerosol composition measurements and ECMWF simulations (LTS and large-scale vertical velocity) and integrated over 1-min time intervals. This means that the aerosol composition and LTS (vertical velocity) in the 1-min resolution datasets are assumed to remain constant within 30-min and 1-hour time periods, respectively.

We have added the sentence "To investigate the influence of aerosols on cloud properties, aerosol properties (N_a, σ_s, composition), cloud properties (COD, LWP, DER, boundary-layer height), surface meteorological parameters, and ECMWF simulations (LTS, large-scale vertical velocity) were matched according to observation time and averaged and interpolated over 1-min time intervals. " to the revised manuscript.

4. Page 7, Line 23-25. For Spring season, AE values generally lower than other season, especially for April and May as shown in Figure 3 and Table 1. Also, σ1/σ10 value is lowest in Spring. Which indicates aerosol plumes more enriched by larger particles, relatively. Please provide more evidences or paper citations to support the statement "due to the presence of a great number of smaller particles. . .".

Response: We found that this statement is not fully supported by the current dataset and analysis. We have thus removed the sentence "The largest values of N_a corresponding to moderate values of σ_s are found in spring and are likely due to the presence of a greater number of smaller particles with less optical sensitivity."

5. Page 8, Line 2-6. Please specify the exact months in this argument, and how to conclude that "This indicates that strong surface. . ."

Response: We have added the specific months to the sentence: "Months in summer and winter with the strongest mean surface wind speeds (e.g., June and January/February, respectively) …". The next sentence is not fully supported by the current dataset and analysis, so we have removed the "This indicates that strong surface …" sentence.

6. Page 8, Line 25. Why only data of July and August 2012 are shown? How about particle size distribution in Spring and Autumn, since they are argued in section 3.1.1 as having discrepancies between Na and σ due to particle size distributions.

Response: Here, we intended to examine the relationship between particle size and particle chemical composition. However, data were not available in spring and autumn.

7. Page 9, Line 1. Please specify the bin sizes used for low and high AI condition. Is there any reason for the mismatched bins between those two conditions, as shown in Figure 7?

Response: We have added the sentence "The cloud properties were averaged over each 6-K LTS bin from 0 K to 30 K under low and high scattering AI conditions."
The x-axis represents the mean values of LTS in each LTS bin. This is the reason for the mismatched bins between the two conditions.

8. Page 10, Line 8. "positive correlation each other" should be "positive correlation between each other".

Response: The sentence has been changed to "The changes in DER with LTS possibly reflect the changes in LWP with LTS due to the high positive correlation between LWP and DER (Zhang et al., 2011; Sporre et al., 2014)."

9. Page 11, Line 30. "a narrower PDF a distinct peak" should be "a narrower PDF with distinct peak".

Response: The sentence has been changed to "The high aerosol loading cases, conversely, have narrower PDFs with distinct peaks between 60 and 70 g m^{-2}."

10. Page 12, Line 23-24. How about FIE under cluster III which has occurrence of 21.6%, and how to determine samples are not enough under cluster II.

Response: The air-mass clusters were determined for each day during the observation period. Although 15.9% and 21.6% of the daily trajectories belong to the clusters II and III, the number of combined cloud and aerosol samples passing the screening criteria (as described in section 2.2.2) are insufficient to do such an analysis. Furthermore, only cases with sample numbers greater than 50 and with calculated values of FIE that are statistically significant at the 95% confidence level (P = 0.05) are discussed in the study.
We have added the sentence "Only those cases with sample numbers greater than 50 per bin and where the calculated values of FIE are statistically significant at the 95% confidence level (P = 0.05) are analyzed here." to the revised manuscript.

11. Page 13, Line 5-9. For ground-based assessments of FIE, Kim et al. (2008) and McComiskey et al. (2009) found decrease of FIE with LWP due to enhanced collision coalescence, please provide

the information of cloud droplet number concentration to support the statement “more droplets can get activated”.

Response: Conflicting findings regarding the dependence of the FIE on the LWP have been reported, i.e., a positive correlation in some studies (Pandithurai et al., 2009; Harikishan et al., 2016), a negative correlation in others (Kim et al. 2008; McComiskey et al., 2009; Liu et al., 2016), and an independence of the FIE on the LWP (Lihavainen et al., 2010; Zhao et al., 2012). Different mechanisms have been reported explaining the negative correlation (i.e., a decrease in cloud droplets due to enhanced collision-coalescence) and the positive correlation (i.e., an increase in cloud droplets due to enhanced aerosol activation). Thus, the dependence of the FIE on the LWP likely depends on which mechanism dominates during the study period in question.

Unfortunately, cloud droplet number concentrations were not available during the field campaign, but our results are consistent with some previous studies. The latter mechanism mentioned above possibly plays a dominant role.

Aerosol Properties and Their Influences on Low Warm Clouds during the Two-Column Aerosol Project

Jianjun Liu[1, 2] and Zhanqing Li[2, 3]

[1]Laboratory of Environmental Model & Data Optima, Laurel, MD, USA
[2]Earth System Science Interdisciplinary Center, University of Maryland, College Park, MD, USA.
[3]State Laboratory of Earth Surface Process and Resource Ecology, College of Global Change and Earth System Science, Beijing Normal University, Beijing, China.

Correspondence to: Jianjun Liu (jianjun5212@163.com), Zhanqing Li (zhanqing@umd.edu)

Abstract. Twelve months of measurements collected during the Two-Column Aerosol Project field campaign at Cape Cod, Massachusetts, which started in the summer of 2012, were used to investigate aerosol physical, optical, and chemical properties, and their influences on the dependence of cloud development on thermodynamic (i.e., lower tropospheric stability, LTS) conditions. Relationships between aerosol loading and cloud properties under different dominant air-mass conditions and the magnitude of the first indirect effect (FIE), as well as the sensitivity of the FIE to different aerosol compositions, are examined. The seasonal variation in aerosol number concentration (N_a) was not consistent with variations in aerosol optical properties (i.e., scattering coefficient, σ_s, and columnar aerosol optical depth). Organics were found to have a large contribution to small particle sizes. This contribution decreased during the particle growth period. Under low aerosol loading conditions, the liquid water path (LWP) and droplet effective radius (DER) significantly increased with increasing LTS, but under high aerosol loading conditions, LWP and DER changed little, indicating that aerosols significantly weakened the dependence of cloud development on LTS. The reduction in LWP and DER from low to high aerosol loading conditions was greater in stable environments, suggesting that clouds under stable conditions are more susceptible to aerosol perturbations than those under more unstable conditions. High aerosol loading weakened the increase in DER as LWP increased and strengthened the increase in cloud optical depth (COD) with increasing LWP, resulting in changes in the interdependence of cloud properties. Under both continental and marine air-mass conditions, high aerosol loading can

Deleted: over
Deleted: influence
Deleted:), which suggests that a greater number of smaller particles with less optical sensitivity
Deleted: present. Strong surface winds generally resulted in smaller σ_s and a smaller
Deleted: of fine particles to the total scattering extinction, but resulted in large N_a, suggesting that strong surface winds transported more aerosols with
Deleted: and less optical sensitivity to the site. The large
Deleted: of organics to small particle sizes was observed which
Deleted: For
Deleted: increase
Deleted: for
Deleted: weaken
Deleted: suggesing
Deleted: in a
Deleted: influenced by
Deleted: in
Deleted: the
Deleted: pattern
Deleted: each other

significantly increase COD and decrease LWP and DER, narrowing their distributions. Magnitudes of the FIE estimated under continental air-mass conditions ranged from 0.07±0.03 to 0.26±0.09 with a mean value of 0.16±0.03 and showed an increasing trend as LWP increased. The calculated FIE values for aerosols with a low fraction of organics are greater than those for aerosols with a high fraction of organics. This implies that clouds over regions dominated by aerosol particles containing mostly inorganics are more susceptible to aerosol perturbations, resulting in larger climate forcing, than clouds over regions dominated by organic aerosol particles.

Deleted: made the shift in
Deleted: towards larger values,
Deleted: in
Deleted: towards smaller values, and significantly narrowed the distribution of LWP and DER.
Deleted: condition
Deleted: increase
Deleted: mass
Deleted: dominated cases
Deleted: larger
Deleted: that
Deleted: mass
Deleted: dominated cases, implying
Deleted: containing mainly organics
Deleted: .

1 Introduction

Aerosols can significantly influence climate change through their direct and indirect effects (IPCC, 2013; Li et al., 2016, 2017). The aerosol direct effect is when aerosol particles change Earth's radiative balance by scattering and absorbing solar radiation (e.g., Liu et al., 2012; X. Yang et al. 2016, 2018). The aerosol indirect effect is when aerosols change cloud microphysical, macrophysical, and precipitation properties through their role as cloud condensation nuclei (CCN) or ice nuclei (IN). Under constant liquid water path (LWP) conditions, an increase in aerosol concentration will lead to an increase in CCN concentration. This results in an increase in cloud droplet number concentration, a decrease in the cloud droplet effective radius (DER), and a more reflective cloud. This is referred to as the first aerosol indirect effect (FIE) (Twomey, 1977; Feingold et al., 2003; Garrett et al., 2004; Zhao et al., 2018, 2019). The decrease in DER will reduce the chances of precipitation forming, which prolongs the lifetime of a cloud and enhances its LWP. This is known as the second aerosol indirect effect (e.g., Albrecht, 1989). Aerosols also influence cloud properties through the thermal emissivity effect (e.g., Garrett and Zhao, 2006; Zhao and Garrett, 2015) and the semi-direct effect (e.g., Koren et al., 2004). Estimates of indirect aerosol effects have large uncertainties (Boney and Dufresne, 2006; Lohmann et al., 2010). This makes the impact of aerosols on the prediction of the current and future behaviors of Earth's climate system highly uncertain (McComiskey et al., 2008; IPCC, 2013).

Moved (insertion) [1]
Deleted: .
Deleted:).
Deleted: .
Deleted: behavior

The observed response of warm low cloud properties to aerosol properties has been observed from satellite-based remote sensing (Bréon et al., 2002; Lebsock et al., 2008; Su et al., 2010; F. Wang et al., 2014), surface-based remote sensing (Kim et al., 2003; Feingold et al., 2003; Garrett et al., 2004; Feingold et al., 2006; McComiskey et al., 2009; Liu et al., 2016; Qiu et al., 2017; Liu et al., 2018a), combined surface measurements and satellite retrievals (Sporre et al., 2012, 2014),

and aircraft measurements (Zhang et al., 2011; Twohy et al., 2013; Painemal and Zuidema, 2013; Werner et al., 2014; Zhao et al., 2018, 2019; Y. Yang et al., 2019). Most of these studies have shown that DER significantly decreases as aerosol loading increases. However, LWP can increase or decrease with aerosol loading, depending on cloud thermodynamics and dynamics (Han et al., 2002). Current estimates of FIE from all available observational platforms have a large range of values because each set of measurements used has its own set of uncertainties, and so do their approaches. The large uncertainty and the wide range of FIE values result in large uncertainties in aerosol indirect radiative forcing estimates (McComiskey and Feingold, 2008). Narrowing uncertainties in measures of aerosol-cloud interactions (ACI) and developing well-constrained parameterizations for models requires analyses of ACI over different climatic and aerosol regions of the earth.

Large-scale thermodynamic conditions, such as lower tropospheric stability (LTS), significantly influences cloud development. Changes in ACI due to different LTS have been widely investigated using observations made from the surface and from satellite remote sensing (Matsui et al., 2004; Su et al., 2010; Liu et al., 2016). However, to what degree the dependence of cloud development to aerosol perturbations are related to large-scale dynamic thermodynamic conditions is not well known. Moreover, the mechanism behind the aerosol FIE is that aerosols affect the cloud droplet number and the cloud DER through their role as CCN, which is determined by the aerosol particle size, number concentration, chemical composition, amount of water vapor, and meteorology (Sekiguchi et al., 2003; J. Wang et al., 2008; Qiu et al., 2017; Yang et al., 2019). Liu and Li (2018b) reported a significant influence of aerosol hygroscopicity on the magnitude of the aerosol FIE when aerosol optical quantities are used to estimate the FIE. The role of aerosol size and number concentrations on the FIE has also been examined (Garrett et al., 2004; Komppula et al., 2005; Anttila et al., 2009). Garrett et al. (2004) indicated a weak sensitivity of FIE to aerosols with small particle sizes but a stronger sensitivity to aerosols with relatively large sizes. However, the question of how sensitive cloud properties are to aerosol composition in addition to aerosol loading is still under investigation (Hao et al., 2013; Portin et al., 2014).

The Department of Energy's Atmospheric Radiation Measurement (ARM) mobile facility was stationed at Cape Cod, Massachusetts from July 2012 to June 2013 for the Two-Column Aerosol Project (TCAP) field campaign (Berg et al., 2016). Measurements of aerosol, radiation, and cloud characteristics were made at the site, which is subject to both clear and cloudy conditions

Deleted: as well as by
Deleted:).
Deleted: the above
Deleted: with increases in
Deleted: measurement approach
Deleted: .
Deleted: in estimates
Deleted: the
Deleted: results
Deleted: a
Deleted: uncertainty
Deleted: Cloud development is significantly influenced by
Deleted:).
Deleted: as
Deleted: changes
Deleted: droplet effective radius (
Deleted:)
Deleted: and
Deleted: (Menon et al., 2002;
Deleted:).
Deleted: was reported (
Moved up [1]: Liu et al.,
Deleted: 2018b).
Deleted:), whereas

as well as clean and polluted conditions. Continental, marine, and continental-marine mixed air masses commonly pass over the site. This study uses data collected during the TCAP field campaign to investigate aerosol physical, optical, and chemical properties, and their influence on the dependence of cloud development on large-scale thermodynamic conditions under different air-mass conditions. Also investigated is the influence of aerosol loading on cloud properties under different air-mass conditions and the magnitude of the FIE, as well as the sensitivity of the FIE to different aerosol compositions and aerosol loadings. Section 2 describes the data and methods used in this study. Section 3 presents the seasonal variations in aerosol physical, optical, and chemical properties and their influence on low, warm clouds. Section 4 gives conclusions.

2 Data and methods

2.1 Aerosol properties

2.1.1 Surface aerosol properties

The optical properties of surface aerosols were measured by a suite of instruments making up the Aerosol Observation System (AOS), which is the primary ARM platform for in situ aerosol observations. The TSI-3010 condensation particle counter was used to obtain the total number concentration of condensation particles (N_a) with diameters larger than 10 nm and smaller than 3 μm. A TSI-3653 nephelometer and a Radiance Research particle soot absorption photometer (PSAP) measured the scattering (σ_s) coefficients at three wavelengths (450, 550, and 700 nm) and the absorption (σ_a) coefficients at three wavelengths (470, 528, and 660 nm), respectively, of total (≤ 10 μm) and fine-mode (≤ 1 μm) aerosol particles (Jefferson, 2011). Nephelometer and PSAP measurements have undergone calibration and quality control using the methods developed by Anderson and Ogren (1998) and Anderson et al. (1999), respectively. Measurements of σ_a at 470 nm were normalized to 450 nm to match σ_s measurements. The single-scattering albedo (SSA) of surface aerosol particles is then calculated as $\sigma_s/(\sigma_s+\sigma_a)$ using σ_s and σ_a at 450 nm. The time resolution of the N_a, σ_s, and σ_a measurements is one minute.

The aerosol size distribution ranging from 15 nm to 450 nm was measured by a scanning mobility particle sizer (SMPS) with five-minute averaging. The SMPS contains a cylindrical differential mobility analyzer (TSI Inc., model 3081) and a condensation particle counter (TSI Inc., model 3010) and is calibrated using polystyrene latex standards (J. Wang et al., 2003). An aerosol chemical speciation monitor (ACSM) measured the bulk chemical composition of the non-

Deleted: The site is commonly influenced by different air-masses, such as the
Deleted: mass.
Deleted: the
Deleted: masses influenced.
Deleted: ,
Deleted: question of how
Deleted: in addition to
Deleted: loading, are also investigated.
Deleted: are described in section 2.
Deleted: are presented in section 3. Conclusions are given in
Deleted: greater
Deleted: . The scattering (σ_s)
Deleted: absorption (σ_a) coefficients of total (≤ 10 μm) and fine mode (≤ 1 μm) aerosol particles were measured under dry conditions with a relative humidity (RH) level equal to 40% using
Deleted: at three wavelength (450, 550, and 700 nm) and
Deleted: ;
Deleted: been calibrated
Deleted: controlled
Deleted: TSI (
Deleted: was

refractory components of sub-micron (aerodynamic diameter ranging from ~40 to 1000 nm) aerosol particles (organics, sulfate, nitrate, ammonium, and chloride). The ACSM is a thermal vaporization electron impact ionization mass spectrometer built upon the same technology as the widely used aerosol mass spectrometer. Under ambient conditions, the detection limit of the mass concentration of particles is less than 0.2 μg m^{-3} for 30-minute signal averaging. The ACSM is calibrated with ammonium nitrate following the method of Ng et al. (2011).

Deleted: =
Deleted: -
Deleted:) was measured by an aerosol chemical speciation monitor (ACSM), which
Deleted: ,
Deleted: build
Deleted: detect limitation
Deleted: concentrations
Deleted: /m^3

2.1.2 Columnar aerosol properties

Columnar aerosol optical depths (AODs) and Angstrom exponents (AEs) were obtained from the Aerosol Robotic Network (AERONET) database (Holben et al., 1998). AODs are retrieved from direct Sun measurements with an uncertainty of 0.01–0.02 (Eck et al., 1999). This study uses Level 2.0 quality-assured and cloud-screened data.

Deleted: AOD
Deleted: AE
Deleted: -
Deleted: In
Deleted: ,
Deleted: was used

2.2 Cloud properties

2.2.1 Cloud boundaries

Cloud-base and cloud-top heights were identified using a combination of observations from the 95-GHz W-band ARM cloud radar (WACR), the micropulse lidar (MPL), and the ceilometer (Kollias et al., 2007). The algorithm used in the cloud boundary retrieval is similar to the method developed by Clothiaux et al. (2000) based on 35-GHz millimeter cloud radar observations. Cloud and precipitation masks are determined from the WACR based on the signal-to-noise ratio thresholds determined for each time profile. An MPL cloud mask is combined with ceilometer cloud-base estimates to produce a best-estimate cloud base for each time point. The MPL and WACR cloud masks are then merged with an additional filter to remove insect returns in the lower troposphere. Insects are identified using a combination of WACR linear depolarization ratio and reflectivity measurements. The temporal and vertical resolutions of the cloud boundary product are 5 sec and 42.856 m, respectively. Cloud-base and cloud-top heights were temporally averaged to generate data at a 1-min time resolution. The cloud-base and cloud-top height uncertainties are ~7.5 m and ~45 m, respectively (Zhao et al., 2012a; Garrett and Zhao, 2013).

Deleted:), which is
Deleted: The WACR
Deleted: mask is derived
Deleted: -
Deleted: , and then
Deleted: filtering of the resulting cloud mask is done
Deleted: to remove insect returns
Deleted: resolution
Deleted: is
Deleted: seconds

2.2.2 Cloud microphysical properties

A two-channel narrow field-of-view (NFOV) radiometer and a microwave radiometer profiler (MWRP) generated cloud optical depth (COD) and LWP retrievals. The cloud droplet effective radius (r_e) was calculated using the following equation:

$$\tau = \frac{3LWP}{2\rho_w r_e}$$

where ρ_w is the density of liquid water, and τ is the COD in the visible. The NFOV radiometer with a 5.7° field of view measuring downwelling zenith radiances at 673 nm and 870 nm at a 1-s time resolution is used to retrieve COD using the method described by Chiu et al. (2010) and Liu et al. (2013). Simultaneous highly accurate AERONET sunphotometer-measured radiances (Holben et al., 1998) quantified the biases in the NFOV radiance measurements (Fig. 1). AERONET and NFOV radiances agree well at 673 and 870 nm (coefficient of correlation, r, equal to 0.99 in both cases). However, NFOV-measured zenith radiances at 673 nm are underestimated by ~15%. Consequently, NFOV measurements at 673 nm were adjusted using the following formula:

$$F_{673,adj} = 1.1519 * F_{673,obs} + 0.0007$$

where $F_{673,obs}$ represents measured zenith radiances, and $F_{673,adj}$ represents adjusted radiances at 673 nm. The total uncertainty in COD retrievals using this method is ~17% (Chiu et al., 2010). The COD retrievals were averaged to generate data at a 1-min resolution for matching the time resolution of the LWP retrievals. The MWRP built by the Radiometrics Corporation measures atmospheric brightness temperatures at 12 frequencies. LWPs were retrieved using brightness temperatures measured at the five K-band channels (22.235, 23.035, 23.835, 26.235, and 30.0 GHz) with a 1-min time resolution based on the statistical retrieval algorithm developed by Liljegren et al. (2004). Typical uncertainties in LWP retrievals from microwave radiometers is ~20 g m^{-2} for LWP < 200 g m^{-2} and ~10% for LWP > 200 g m^{-2} (Liljegren et al., 2004; Dong et al., 2008).

This study considers only non-precipitating, low, warm clouds with cloud-top heights less than 3 km. LWP observations less than 40 g m^{-2} and greater than 300 g m^{-2} were excluded to avoid very thin clouds, broken cloud cover, post-precipitation conditions (McComiskey et al., 2009), and potential precipitation contamination (Dong et al., 2008).

2.3 Surface and large-scale meteorological parameters

Deleted: Cloud optical depths (COD) and liquid water paths (LWP) were retrieved based on measurements from

Deleted:).

Deleted: .

Deleted: -

Deleted: -

Deleted: , which

Deleted: retrieved

Deleted: radiance measurements with a high accuracy from the

Deleted: Sun photometer

Deleted: were used to quantify

Deleted: R=

Deleted: a

Deleted: The typical uncertainty

Deleted: Dong et al., 2008;

Deleted: In

Deleted: ,

Deleted: precipitation

Deleted: height

Deleted: are considered. The

Deleted: or

Deleted: as well as

Deleted:)

The ARM surface meteorological system measured surface meteorological parameters during the campaign period at a 1-min resolution. The large-scale vertical motion (ω) at 700 hPa and LTS are used in this study to constrain large-scale dynamic and thermodynamic conditions (Su et al., 2010; Medeiros and Stevens, 2011; Liu et al., 2016). The difference between the potential temperature of the free troposphere (700 hPa) and the surface defines LTS.

To investigate the influence of aerosols on cloud properties, aerosol properties (N_a, σ_s, composition), cloud properties (COD, LWP, DER, boundary-layer height), surface meteorological parameters, and ECMWF simulations (LTS, large-scale vertical velocity) were matched according to observation time and averaged and interpolated over 1-min time intervals.

2.4 Air-mass trajectory classification

Two-day air-mass back trajectories arriving at the site at 500 m at midnight were simulated using the Hybrid Single Particle Lagrangian Integrated Trajectory model (Stein et al., 2015; Rolph, 2016). All simulated trajectories are classified into three clusters. Cluster I represents continental air masses generally originating from the continental area located to the west of the site and moving over the site. Air masses originating from the ocean area to the east of the site and directly moving over the site are the marine air masses (cluster II). Cluster III represents an air mass that has passed over both continental regions and the ocean to the site, influenced by anthropogenic and marine aerosols. During the study period, the occurrence frequencies of cluster I, II, and III air masses were 62.5%, 15.9%, and 21.6%, respectively.

3 Results

3.1 Variations in aerosol properties

3.1.1 Seasonal variations in aerosol optical properties and number concentration

Figure 2 shows monthly statistics describing surface-measured σ_s for total (σ_{10}) and fine-mode (σ_1) aerosol particles and N_a. Table 1 summarizes their seasonal and annual mean values. Maxima in σ_1 and σ_{10} are found in the summer months, and minima in σ_1 and σ_{10} are found in the winter months. Fine particles dominate aerosol scattering in the summertime and are responsible for ~75% of the total particle scattering. The contribution of fine particle scattering to total particle scattering in other seasons ranges from ~46% to ~54%, indicating that particles with diameters ≤ 1 μm and ranging from 1 to 10 μm play a similar role in aerosol scattering extinction. Monthly

Deleted: were measured by the ARM surface meteorological system …
Deleted: minute
Deleted: is
Deleted: LTS is calculated as
Deleted: . Values of ω and potential temperature were obtained from the European Centre for Medium Range Weather Forecasts model runs for ARM analysis with a one-hour resolution for a 0.56° x 0.56° box centered on the site.
Deleted: trajectories
Deleted: HYSPLIT
Deleted:), and
Deleted: the
Deleted: -
Deleted: , which
Deleted: originated
Deleted: at
Deleted: moved
Deleted: The air-
Deleted: which originated
Deleted: of
Deleted: moved to
Deleted: identified
Deleted: -
Deleted: And the
Deleted: -
Deleted: with
Deleted: aerosol influenced.
Deleted: -
Deleted: was
Deleted: %
Deleted: show
Deleted: are summarized in Table 1.
Deleted: sizes
Deleted: -

and seasonal variations in N_a show that maximum and minimum seasonally mean N_a values occur in spring and autumn, respectively, inconsistent with the variations in aerosol scattering coefficient. This inconsistency is probably due to seasonal differences in aerosol particle size distribution and chemical composition since aerosol extinction properties depend strongly on particle size and chemical composition. The total particle SSA shows a slight seasonal variation, suggesting smaller changes in aerosol particle absorption properties. Figure 3 shows monthly statistics describing columnar AOD and AE. Table 1 summarizes their seasonal and annual mean values. The variations in AOD and AE are consistent with the variations in surface-measured σ_s and the ratio σ_1/σ_{10}, indicating that surface aerosol properties can represent columnar aerosol properties very well at this site. Figure 4 shows monthly mean wind speeds and wind directions during the campaign period. Monthly mean wind speeds ranged from ~3.8 m s^{-1} to 6.6 m s^{-1}, and southwesterly winds dominated throughout the whole year over the area. Months in summer and winter with the strongest mean surface wind speeds (e.g., June and January/February, respectively) are generally times when the contribution of fine particles to the total scattering extinction is small.

3.1.2 Aerosol optical properties under different air-mass conditions

Table 2 gives the discrepancies in aerosol properties when different air masses are in place over the site. The mean value of σ_1 is the largest/smallest under continental/marine air-mass conditions. However, σ_{10} is the largest under cluster III conditions and has similar values under cluster I and II conditions. The inconsistent variations in σ_1 and σ_{10} under different air-mass conditions can be explained by dominant particle size as indicated by the ratio σ_1/σ_{10}. When the continental air-mass influenced the site, fine particles dominated aerosol scattering and were responsible for ~65% of the total particle scattering, indicating that more anthropogenic aerosols with small particle sizes were transported to the site from continental regions to the west. The values of σ_1/σ_{10} under cluster II and III air-mass conditions show that both fine-mode and coarse-mode particles played similar roles on the total particle scattering. The variation in N_a is consistent with that in σ_1 with the largest and smallest values under cluster I and II conditions, respectively. Smaller SSA values are found under continental air-mass conditions, suggesting that more absorbing aerosols were present in this air mass than in other air masses due to the anthropogenic influence. AOD values in each air mass are similar, and the variation in AE is consistent with the variation in the ratio σ_1/σ_{10}.

Deleted: seasonal…easonally mean N_a occurs…alues occur in spring and autumn, respectively, which is not consistent…nconsistent with the variations in aerosol scattering coefficient. This inconsistency is probably due to the difference…easonal differences in aerosol particle size distribution in each season…nd chemical composition since aerosol extinction properties significantly …epend strongly on particle size. The values of N_a corresponding to moderate values of σ_s are found in spring and are likely due to the presence of a greater number of smaller particles with less optical sensitivity…and chemical composition. The total particle SSA shows a slight seasonal variation, suggesting smaller changes in aerosol particle absorption properties. Figure 3 shows monthly statistics describing columnar AOD and AE. Table 1 summarizes their seasonal and annual mean values are summarized in Table 1…. The variation…ariations in AOD and AE is…re consistent with the variation…ariations in surface-measured σ_s and the ratio σ_1/σ_{10}, indicating the…hat surface aerosol properties can represent the …olumnar aerosol properties very well at this site. Figure 4 shows monthly mean wind speeds and wind directions during the campaign period. Monthly mean wind speeds ranged from ~3.8 m /…$^{-1}$ to 6.6 m /…$^{-1}$, and southwesterly winds dominated throughout the whole year over the area. Months in summer and winter with the strongest mean surface wind speeds (e.g., June and January/February, respectively) are generally have small σ_s with a small …imes when the contribution of fine particles to the total scattering extinction. However, relatively large aerosol number concentrations were measured. This indicates that strong surface wind speeds transported smaller aerosol particles with no optical sensitivity from the continental interior to over the site. ... [1]

Deleted: masses

Deleted: gave…ives the discrepancies in aerosol properties when different air -…asses influenced on…re in place over the site. The mean value of σ_1 is the largest/smallest under the …ontinental/marine air-mass conditions;… However, σ_{10} is the largest under cluster III condition…onditions and shows…as similar values under cluster I and II conditions. The inconsistent variations in σ_1 and σ_{10} under different air-mass conditions are due to the particles with different …an be explained by dominant particle size dominated, …s indicated by the ratio σ_1/σ_{10}. When the continental mass influenced the site, the …ine particles dominate…ominated aerosol scattering and are…ere responsible for ~65% of the total particle scattering, indicating the…hat more anthropogenic aerosols with small particle size are…izes were transported to the site from continental regions to the west. The values of σ_1/σ_{10} under cluster II and III air-mass conditions show that the…oth fine-mode and coarse-mode particles play the…layed similar role…oles on the total particle scattering. The variation in N_a is consistent with that in σ_1 with the largest and smallest values under cluster I and II conditions, respectively. Smaller SSA values are found under continental air-mass conditions suggested the … suggesting that more absorbing aerosols are found…ere present in this air mass than that under…n other air -…asses conditions …ue to the anthropogenic influence. The variation in …OD under…alues in each air -…ass condition shows the…re similar values ... [2]

3.1.3 Aerosol chemical composition and size distribution

Figure 5 shows the size distribution and the corresponding mass fraction of organics, sulfate, ammonium, and nitrate of surface aerosol particles sampled in July and August 2012. New particle formation and growth periods were detected and are outlined by red rectangles in the figure. During the measurement period, fine particles containing more organics were dominant with a mean particle radius of 91.4±20.6 nm and a mean organic mass fraction of 0.67±0.16. Mean mass fractions of sulfate, ammonium, and nitrate are 0.18±0.11, 0.10±0.09, and 0.04±0.02, respectively. At the beginning of new particle formation and growth periods, organics contributed the most to small particle sizes. Their contribution decreased as the growth period progressed to be replaced by contributions from inorganics, in particular, sulfate. This is possible because sulfate ions are formed during nucleation involving neutral gaseous species like ammonia and sulfuric acid (Crilley et al., 2014). Small aerosol particles generally contribute more organics to the total aerosol mass over the study site, which can also be seen in the relation between mean aerosol particle radii and organic mass fraction (Fig. 6). The strong decrease in aerosol particle size with increasing organic mass fraction has also been reported by others (Broekhuizen et al., 2006; McFiggans et al., 2006).

Deleted: Figure 5

Deleted: contribute

Deleted: decreases

Deleted: with

Deleted: increase in

3.2 Aerosol, cloud, and meteorological conditions

3.2.1 Aerosol effects on the dependence of cloud properties on meteorological conditions

Low, warm cloud properties are sensitive to changes in thermodynamic conditions (Su et al., 2010; Medeiros and Stevens, 2011; Liu et al., 2016). Figure 7 shows cloud properties (LWP and DER) as functions of LTS under low and high scattering aerosol index (AI) conditions for continental and marine air masses. The scattering AI here is used as a proxy for CCN (Liu and Li, 2014; Sena et al., 2016) and is defined as the product of surface-measured aerosol scattering coefficients and surface-measured scattering Ångström exponents. Low and high scattering AIs are defined as the lowest and highest quarter of all scattering AI samples, respectively. The cloud properties were averaged over each 6-K LTS bin from 0 K to 30 K under low and high scattering AI conditions. The differences in meteorological parameters (e.g., temperature, wind speed, and relative humidity) at the surface and at 850 hPa, and in large-scale dynamic (ω) and thermodynamic parameters (LTS) are not significant under low and high scattering AI conditions (figure not shown). Table 2 summarizes the means and standard deviations of cloud properties

Deleted: the

Deleted: ,

Deleted: a function

Deleted: -mass conditions. In this study,

Deleted: the CCN

Deleted: (Nakajima et al., 2001;

Deleted:), which

Deleted: multiple by

Deleted: angstrom

Deleted: AI

Deleted: (the same hereinafter). The

Deleted: the

Deleted: such as

Deleted: etc.)

Deleted: ,

Deleted: for the

Deleted: summarized

Deleted: mean

Deleted: deviation

under each air-mass condition. Clouds influenced by marine air mass conditions (cluster II) have the largest COD, LWP, and DER (33.0±18.3, 243±197 g m^{-2}, and 10.9±6.6 μm, respectively), and clouds associated with the air mass from continental areas (cluster I) have the smallest cloud properties (COD = 25.7±14.5, LWP = 127±99 g m^{-2}, and DER = 7.9±4.8 μm). The top panels of Fig. 7 show that LWP significantly increases with increasing LTS under low aerosol conditions, consistent with results from studies using surface-based measurements (e.g., Liu et al., 2016), satellite measurements (e.g., Su et al., 2010), aircraft measurements (e.g., Cecchini et al., 2016), and model simulations (e.g., Johnson et al., 2004; West et al., 2014). Johnson et al. (2004) showed that an increase in stability induces increases in the buoyancy of free-tropospheric air above the temperature inversion capping the boundary later, inhibiting the entrainment of dry air through the cloud top and increasing LWP as a result. Under high aerosol conditions, LWP changes little as LTS increases. A likely reason is inhibited cloud droplet sedimentation due to the reduced cloud droplet size, enhancing evaporation and entrainment at the cloud top and reducing LWP (Kaufman et al., 2005; Hill et al., 2009; Zhao and Garrett, 2015; Liu et al., 2016). There are similar variations in DER with increasing LTS under low and high aerosol conditions (bottom panels of Fig.7), i.e., increasing DER as LTS increases under less polluted conditions and almost constant DER as LTS increases under more polluted conditions. The changes in DER with LTS possibly reflect the changes in LWP with LTS due to the high positive correlation between LWP and DER (Zhang et al., 2011; Sporre et al., 2014). The enhanced LWP under highly stable conditions can supply the water needed for cloud droplet growth (Su et al. 2010; Zhang et al. 2011). The increase in LWP is also commonly accompanied by an increase in droplet collision–coalescence, resulting in a decrease in cloud number concentration, thus leading to an increase in DER (Kim et al., 2008; McComiskey et al., 2009; Liu et al., 2016; Zhao et al., 2018, 2019; Y. Yang et al., 2019). Differences in LWP and DER between low and high LTS conditions are larger under low pollution conditions than under high pollution conditions. This suggests that high aerosol concentrations can significantly weaken the thermodynamic influence on the increase in LWP and DER due to the aerosol perturbation. These results imply that the development of clouds in a highly polluted environment is inhibited even though the thermodynamic conditions may be the same as those in a much less polluted environment. The chances of precipitation are thus reduced because the rainfall frequency of warm, low clouds and LWP are highly correlated (Chen et al., 2011; Liu et al., 2013).

Deleted: under the
Deleted: and
Deleted: with
Deleted: of
Deleted: of
Deleted: of
Deleted: .
Deleted: condition, which is
Deleted: those
Deleted: .
Deleted:)
Deleted: .
Deleted: .
Deleted: as well
Deleted: .
Deleted: The
Deleted: simulations indicated
Deleted: increasing
Deleted: can induce the
Deleted: -
Deleted: , resulting in the increases in
Deleted: change
Deleted: The lower LWP under more aerosol conditions possibly because the…
Deleted: likely enhances
Deleted: , resulting in a reduction in
Deleted: .
Deleted: and Feingold
Deleted: Similar with the
Deleted: LWP with LTS, the
Deleted: under both air-masses conditions shows significant increases with increasing LTS under less polluted condition and.. [3]
Deleted: condition
Deleted: can possible because
Deleted: each other
Deleted: And
Deleted: the
Deleted: ,
Deleted: .
Deleted: .
Deleted: The
Deleted: under the similar thermodynamic conditions,
Deleted: , which reduces
Deleted: is
Deleted: with LWP

For all LTS bins, clouds under high aerosol conditions have lower values of LWP and DER than clouds under low aerosol conditions. The reduction in LWP and DER is greater in stable environments than in unstable environments, suggesting that clouds in stable environments are more affected by the aerosol perturbation than those in more unstable regimes. Studies on marine warm clouds based on surface measurements have also shown this (Liu et al., 2016).

3.2.2 Aerosol effects on the relationships among cloud properties

Figure 8 shows the dependence of COD and DER on LWP under low and high scattering AI conditions for air-mass clusters I and II. Under high scattering AI conditions, COD increases sharply as LWP increases, while under low scattering AI conditions, COD changes little as LWP increases due to the decrease in DER influenced by the aerosol perturbation (Fig. 8a and 8b). Figures 8c and 8d suggest that the DER is sensitive to LWP. An increase in LWP leads to a significant increase in the size of cloud droplets (Zhang et al., 2011; Sporre et al., 2014). The increase in DER with LWP is more rapid under low scattering AI conditions than under high scattering AI conditions. This is because there is a limit to the size a cloud droplet can reach when a given amount of water is shared among a large number of particles (Zhang et al., 2011). High aerosol loading conditions weaken the increase in DER and strengthen the increase in COD as LWP increases, indicating that aerosols have an impact on the COD-LWP and DER-LWP relationships.

Figure 8 also shows that across all LWP bins, COD is larger and DER is smaller under high scattering AI conditions than under low scattering AI conditions, consistent with the "Twomey" effect. The large differences between COD under low and high scattering AI conditions at high LWP values (Fig. 8a and 8b) and between DER under low and high scattering AI conditions at high LWP values (Fig. 8c and 8d) suggest that when clouds have large LWPs, aerosols further inhibit the growth of cloud droplets. Under high aerosol loading conditions, more aerosol particles are activated into CCN, resulting in a rapid increase in cloud droplet concentration as LWP increases. However, under low aerosol loading conditions, cloud droplet concentrations increase slowly as LWP increases due to the lack of a CCN source, so the size of cloud droplets increases rapidly as LWP increases (Zhang et al., 2011).

3.3 Aerosol effect on cloud properties

Deleted: Meanwhile,
Deleted: ,
Deleted: , which is consistent with the
Deleted: the
Deleted: relationship
Deleted: .
Deleted: b). Figure
Deleted: suggests
Deleted: can influence
Deleted: pattern of
Deleted: Figures
Deleted: which is
Deleted: b
Deleted: d) suggests
Deleted: will tend to
Deleted: more. This can happen because
Deleted: and
Deleted: concentrations will increase rapidly
Deleted: the

3.3.1 Variations in cloud properties with aerosol loading under different air-mass conditions

Figure 9 shows the probability distribution functions (PDFs) of COD, LWP, and DER under low and high scattering AI conditions for air mass clusters I and II. Numbers written in each panel are the mean percentage differences in each cloud property defined as $(M_{ch} - M_{cl})/M_{cl} * 100\%$, where M_c represents the mean value of a cloud property and subscripts h and l represent high and low scattering AI levels, respectively. The PDFs of COD, LWP, and COD under high and low scattering AI conditions differ significantly for both air masses. Although the peak values of COD under low and high aerosol loading conditions are similar, clouds under more polluted conditions have more large values of COD than those under less polluted conditions. There are 24.2% and 21.9% increases in COD for cluster I and II respectively. For the low aerosol loading case, the PDF of LWP shows a broad maximum with values from 50 to 180 g m^{-2} (Fig. 9c) and 80 to 230 g m^{-2} (Fig. 9d) for cluster I and II air masses, respectively. The high aerosol loading cases, conversely, have narrower PDFs with distinct peaks between 60 and 70 g m^{-2}. Under high scattering AI conditions, the LWP decreases on the order of 30% and 45% from their values under low scattering AI conditions for the cluster I and II air masses, respectively. Under both air-mass conditions, there is a sharp shift in DER towards smaller values when going from high aerosol loading conditions to low aerosol loading conditions. Under low aerosol loading conditions, the DER values show a broad range with generally higher values varying between 5 and 12 μm for the cluster I air mass and peaking around 15 μm for the cluster II air mass. Under high aerosol loading conditions, the PDF of DER for both air masses is significantly narrower with most of the values less than 10 μm and with peak values around 5 μm. From low to high aerosol loading conditions, DER decreases ~40% (for cluster I) and ~55% (for cluster II). As mentioned before, whether low or high scattering AI conditions are in place, meteorological parameters and large-scale dynamic and thermodynamic parameters show little difference, suggesting that aerosols are responsible for the changes in cloud properties. In general, clouds in a marine air mass have slightly larger decreases in LWP and DER from low to high aerosol loading than those in a continental air mass.

3.3.2 Aerosol first indirect effect

The aerosol FIE is generally quantified as

$$FIE = -\frac{dln(DER)}{dln(\alpha)}|_{LWP},$$

Deleted: cluster…lusters I and II are shown in Fig. 9. ... [4]

Deleted: conditions…evels, respectively. The figure shows that …he PDFs of COD, LWP, and COD under high and low scattering AI conditions differ significantly under…or both air -…asses conditions… Although the peak value…alues of COD is similar …nder low and high aerosol loading conditions are similar, clouds under more polluted conditions have more large values of COD than that…hose under less polluted conditions with enhancement in COD from low to high aerosol loading of … There are 24.2% and 21.9% increases in COD for cluster I and II air-mass, …espectively. For the low aerosol loading case, the PDF of LWP shows a broad maximum with values between…rom 50-…to 180 g m^{-2} (Fig. 9c) and 80-…to 230 g m^{-2} (Fig. 9d) for cluster I and II air-mass…masses, respectively. The high aerosol loading cases, conversely, has a…ave narrower PDF a…DFs with distinct peak at …eaks between 60-…and 70 g m^{-2}. Under high scattering AI conditions, the LWP decreases on the order of 30% and 45% from their values under low scattering AI conditions for the cluster I and II air-mass…masses, respectively. Under both air-masses…ass conditions, there is a sharp shift in DER towards smaller values under…hen going from high aerosol loading conditions than that…o low aerosol loading conditions. Under low aerosol loading conditions. Under low polluted conditions, … the DER values show a broad range and…ith generally higher values with most observations …arying between 5-…and 12 μm for the cluster I air -…ass and peak…eaking around 15 μm for the cluster II air -…ass cases, respectively. For… Under high polluted case…erosol loading conditions, the PDF of DER for both air -…asses conditions…is significantly narrower and…ith most of the values smaller…ess than 10 μm and with peak values around 5 μm. The large difference in …rom low to high aerosol loading conditions, DER under high and low aerosol loading conditions with value of …ecreases ~40% and 55% are founded …for cluster I) and ~55% (for cluster II air-mass, respectively….. As indicated above, the…entioned before, whether low or high scattering AI conditions are in place, meteorological parameters and large-scale dynamic and thermodynamic parameters showed no significant differences for low and high AI conditions indicating…how little difference, suggesting that aerosols are responsible for the changes in cloud properties are mainly contributed to aerosols. Generally… In general, clouds under…n a marine air -…ass conditions…have slightly larger decreases in LWP and DER from low to high aerosol loading than those under…n a continental air -…ass conditions... [5]

where α represents CCN or CCN proxies. The FIE represents the relative change in mean cloud DER with respect to a relative change in aerosol loading for clouds having the same LWP (Feingold et al., 2003). In some studies, the scattering AI is used as the CCN proxy (Liu and Li, 2014). Cloud samples were categorized according to their LWP values. The LWP bins range from 40 to 200 g m^{-2} in increments of 20 g m^{-2}. The choice of a small increment ensures that the LWP constraint is met in each bin. Since there were not enough samples under cluster II air-mass conditions, only FIE for clouds and aerosols under cluster I air-mass conditions are calculated. Only those cases with sample numbers greater than 50 per bin where the calculated values of FIE are statistically significant at the 95% confidence level (P = 0.05) are analyzed here. Figure 10a shows DER as function of scattering AI for clouds with LWP ranging from 120 to 140 g m^{-2}. It illustrates how the FIE is estimated. There is a significant decrease in DER as the scattering AI increases. For this case, the magnitude of the FIE is 0.26 with an uncertainty of 0.09. Figure 10b shows the magnitudes and uncertainties of FIE calculated in each LWP bin. Numbers above each bar are the number of samples that went into the calculation of the FIE in each LWP bin. The magnitude of the FIE changes from 0.07±0.03 to 0.26±0.09 with the smallest value found in the LWP bin of 40–60 g m^{-2} and the largest value found in the LWP bin of 120–140 g m^{-2}. The mean value of FIE during the study period based on all LWP bins is 0.16±0.06. The values of FIE in each LWP bin increase with increasing LWP, especially for LWPs less than 140 g m^{-2}. This is consistent with results from previous studies (e.g., Pandithurai et al., 2009; Sporre et al., 2014; Harikishan et al., 2016). Enhanced aerosol activation due to the increase in LWP may explain this (Zhao et al., 2012b; Painemal and Zuidema, 2013). At higher LWP values, with the availability of more CCN, more droplets can activate. The droplet number increases, but their size decreases at fixed LWP levels (Harikishan et al., 2016). Estimates of the FIE reported from all available platforms range widely and are sensitive to the definition of the aerosol burden (Lihavainen et al., 2010; Zhao et al., 2012b), the methods for retrieving cloud properties (McComiskey et al., 2009), and meteorological conditions such as vertical velocity and atmospheric stability (Feingold et al., 2003; Matsui et al., 2004; McComiskey et al., 2009; Liu et al., 2016; Y. Yang et al., 2019). Theoretical values of the FIE lie between 0 and 0.33 (McComiskey and Feingold, 2008) with most values falling between 0.05 and 0.25 (Zhao et al., 2012b). Based on surface retrievals, Feingold et al. (2003) derived FIE values of 0.02–0.16 with a mean value of 0.10±0.05 for a set of seven cases. In a study using three years of data from the U.S. Southern Great Plains, Kim et al. (2008) found

Deleted: the
Deleted: aerosol index
Deleted: Nakajima et al., 2001;
Deleted: -
Deleted: Due to the lack of
Deleted: for
Deleted: condition, FIE is calculated
Deleted: condition. And only the
Deleted: =
Deleted: discussed in the study.
Deleted: -
Deleted: as an example to explain
Deleted: to estimate
Deleted: in the study. The
Deleted: with increase in
Deleted: is founded
Deleted: are shown in Fig. 10b
Deleted: -
Deleted: -
Deleted: for
Deleted: during the study period.
Deleted: shows an obvious
Deleted: of
Deleted: LWP smaller
Deleted: some of
Deleted: .
Deleted:), can is possibly because the
Deleted: is enhanced
Deleted: of
Deleted: 2012
Deleted: get activated.
Deleted: ,
Deleted: .
Deleted: 2012
Deleted: the
Deleted: -
Deleted: , and

that FIE values ranged from 0.04 to 0.17 over five LWP bins with a mean value of 0.09±0.05. Other estimates of FIE based on surface retrievals have been reported, e.g., 0.07±0.01 for warm, marine boundary-layer clouds over the Azores (Liu et al., 2016), 0.14±0.09 for continental clouds during the monsoon period over a rural continental site in Mahabubnagar, India (Harikishan et al., 2016), and a range of 0.05 to 0.16 over the coastal region at Pt. Reyes, California (McComiskey et al., 2009). The magnitude of the FIE in this study generally falls in this range.

Examined next is the sensitivity of cloud properties to aerosol chemical composition represented by the mass fraction of organics. The aerosol number concentration is used as the CCN proxy here (Li et al., 2011; Yan et al., 2014; Liu et al., 2016) because aerosol scattering coefficient measurements were not taken during the aerosol chemical composition observation period. Three LWP bins were defined: 40–60 g m^{-2}, 60–80 g m^{-2}, and 80–100 g m^{-2}. Figure 11 shows DER as a function of N_a in each LWP bin when aerosol particle mass fractions of organics are low and high. Aerosols with low and high mass fractions of organics are defined as aerosols with mass fractions of organics less than and greater than, respectively, the mean value of the mass fraction of organics of all samples in each LWP bin. Mean values of ω and LTS in each aerosol particle mass fraction of organics category are given in the figure. Differences in ω and LTS between low and high mass fractions of organics are not significant in any LWP bin. FIE estimates when aerosol samples with low mass fractions of organics dominate are 0.10±0.05, 0.15±0.06, and 0.23±0.12 (Fig. 11a-c, respectively), which are greater than the FIE estimates when aerosol samples with high mass fractions of organics dominate (0.07±0.04, 0.12±0.06, and 0.07±0.05, respectively). Clouds are more susceptible to inorganics-dominant aerosol than to organic aerosols, resulting in a greater climate forcing. The mechanism behind the aerosol indirect effect is characterized by the ability of aerosol particles to act as CCN, which is primarily governed by particle size and chemical composition (McFiggans et al., 2006). The cloud-nucleating ability of aerosol particles is significantly greater when the aerosol particles are larger and composed of more inorganic compounds than when they are small and composed of more organic compounds (Dusek et al., 2006; Liu et al., 2011). This study (see Fig. 5) and others have demonstrated that aerosols containing more organic particles are generally smaller than those with more inorganic particles (Broekhuizen et al., 2006; McFiggans et al., 2006; Zhang et al., 2011) and that organic particles are generally less CCN-active than inorganic particles (Raymond and Pandis, 2002; Zhang et al.,

Deleted: at

Deleted: from a 3-year (1999-2001) study at South Great Plain (SGP) in U.S., respectively. The mean

Deleted: value of

Deleted: at

Deleted: at

Deleted: over

Deleted: -

Deleted:) are reported based on the surface-based retrievals.

Deleted: To examine the question of how sensitive are cloud properties to aerosol composition in addition to aerosol loading,

Deleted: was examined.

Deleted: concentrations are

Deleted: here due to the limitation of

Deleted: -

Deleted: -

Deleted: -

Deleted: are shown in Fig. 11.

Deleted: smaller

Deleted: fraction

Deleted: Estimates of the

Deleted: see

Deleted: of the FIE

Deleted: This suggests that clouds under a majority of aerosol particles composed of inorganic compounds conditions

Deleted: perturbations

Deleted: , than clouds under a majority of aerosol particles composed of organic compounds conditions.

Deleted: AIE

Deleted: large

Deleted: are

Deleted: that

Deleted: are

Deleted: .

Deleted: figure

Deleted:),

2011). This can partly explain the smaller FIE values induced by aerosols with large mass fractions of organics.

4 Conclusions

Twelve months (July 2012 – June 2013) of measurements of aerosol and cloud properties, as well as meteorological variables, were acquired during the Two-Column Aerosol Project field campaign at Cape Cod, Massachusetts. The goal of this study is to characterize aerosol physical, optical, and chemical composition properties, and to determine their influences on cloud properties and the dependence of cloud development on large-scale thermodynamic conditions. Also examined was the magnitude of the aerosol FIE and the sensitivities of cloud properties to aerosol composition in addition to aerosol loading.

The maximum and minimum in σ_1 and σ_{10} were found in summer and winter, respectively. Fine particles dominated aerosol scattering in the summer and contributed toward ~75% of the total particle scattering. In other seasons, fine particles contributed toward ~45–54% of the total particle scattering. The maximum and minimum mean values of N_a occurred in spring and autumn, which is not consistent with the variation in σ_s. The variation in AOD is consistent with the variation in surface-measured σ_s and inconsistent with the variation in N_a. This suggests that a large number of particles with less optical sensitivity were present. Months with strong mean surface wind speeds were generally associated with small σ_s and a small contribution of fine particles to the total scattering extinction, but relatively large aerosol number concentrations. This suggests that strong surface winds had ushered in from the inland continental region more optically insensitive aerosols of small particle size. For all new particle formation and growth cases considered in this study, a large contribution of organics to small particles was observed, which then decreased during the particle growth period.

Under low scattering AI conditions, LWP and DER significantly increased as LTS increased, but under high scattering AI conditions, LWP and DER changed little. Differences in LWP and DER between low and high LTS conditions were larger under light pollution than under heavy pollution. This suggests that the dependence of cloud properties is weakened by the aerosol perturbation. The reduction in LWP and DER was greater in stable environments than in unstable environments, indicating that clouds in stable environments are more influenced by aerosol perturbations than those in more unstable regimes. DER significantly increased with increasing

Deleted: conditions
Deleted: collected
Deleted: (TCAP)
Deleted: over
Deleted: influence
Deleted: first indirect effect (
Deleted:)
Deleted: question of how sensitive are
Deleted: were also examined
Deleted: -
Deleted: aerosol scattering coefficient (
Deleted:).
Deleted: aerosol optical depth (
Deleted:)
Deleted: with
Deleted: sizes, which were not optically sensitive.
Deleted: cases representing
Deleted: , indicating that aerosol particles with small sizes generally contribute more organics to the total aerosol mass.
Deleted: increase
Deleted: low
Deleted: conditions
Deleted: high
Deleted: conditions
Deleted: due to

LWP under low aerosol conditions, but slowly increased as LWP increased under high aerosol conditions. Under high scattering AI conditions, COD sharply increased with increasing LWP, but under low scattering AI conditions, the increase was slower. This suggests that aerosols can influence the interdependence of cloud properties.

Analyses of the PDFs of COD, LWP, and DER under low and high aerosol loading conditions in continental airmass (clusters I) and oceanic airmass (clusters II) suggest that high aerosol loading can increase COD and decrease LWP and DER, and narrow the distributions of LWP and DER. The magnitude of FIE estimated under continental air-mass conditions ranged from 0.07±0.03 to 0.26±0.09 with a mean value of 0.16±0.03 and showed an increasing trend as LWP increased. The magnitude of the FIE estimated for aerosols with a low fraction of organics was larger than that for aerosols with a high mass of organics. This suggests that clouds over regions dominated by inorganic aerosols are more susceptible to aerosol perturbations, resulting in larger climate forcing, than clouds over regions dominated by organic aerosols.

Author contributions. JL performed the calculations, analyzed the data, and wrote the paper. ZL contributed to the writing of paper and in scientific discussions of the study.

Competing interests. The authors declare that they have no conflict of interest.

Acknowledgements. The ground-based measurements were obtained from the Atmospheric Radiation Measurement (ARM) program sponsored by the U.S. Department of Energy Office of Energy Research, Office of Health and Environmental Research, Environmental Sciences Division. The study is funded by the DOE/ASE program (DE-SC0018996). The reanalysis data were obtained from the European Centre for Medium-Range Weather Forecasts (ECMWF) model runs for ARM provided by the ECMWF.

Deleted: ,
Deleted: slowly
Deleted: polluted
Deleted: It indicated
Deleted: on
Deleted: pattern
Deleted: between the
Deleted: each other
Deleted: for
Deleted: air mass cluster
Deleted: suggests
Deleted: significantly make the shift in
Deleted: towards larger values,
Deleted: in
Deleted: towards smaller values
Deleted: distribution
Deleted: increase
Deleted: mass
Deleted: were
Deleted: those
Deleted: aerosol particles containing mostly inorganics
Deleted: aerosol particles containing mainly organics
Deleted: has
Deleted: and analyses of
Deleted: research
Deleted: made
Deleted: comments
Deleted: participated
Deleted: discussion
Deleted: (DOE)
Deleted: are

References

Albrecht, B.: Aerosols, cloud microphysics, and fractional cloudiness, Science, 245, 1227–1230, https://doi.org/10.1126/science.245.4923.1227, 1989.

Anderson, T. L., and Ogren, J. A.: Determining aerosol radiative properties using the TSI 3563 integrating nephelometer, Aerosol Sci. Technol., 29, 57–69, https://doi.org/10.1080/02786829808965551, 1998.

Anderson, T. L., Covert, D. S., Wheeler, J. D., Harris, J. M., Perry, K. D., Trost, B. E., Jaffe, D. J., and Ogren, J. A.: Aerosol backscatter fraction and single scattering albedo: measured values and uncertainties at a coastal station in the Pacific Northwest, J. Geophys. Res. Atmos., 104(D21), 26,793–26,807, https://doi.org/10.1029/1999JD900172, 1999.

Anttila, T., Vaattovaara, P., Komppula, M., Hyvärinen, A. P., Lihavainen, H., Kerminen, V. M., and Laaksonen, A.: Size dependent activation of aerosols into cloud droplets at a subarctic background site during the second Pallas Cloud Experiment (2ndPaCE): method development and data evaluation, Atmos. Chem. Phys., 9, 4841–4854, https://doi.org/10.5194/acp-9-4841-2009, 2009.

Berg, L. K., Fast, J. D., Barnard, J. C., Burton, S. P., Cairns, B., Chand, D., Comstock, J. M., Dunagan, S., Ferrare, R. A., Flynn, C. J., et al.: The Two-Column Aerosol Project: Phase I-Overview and impact of elevated aerosol layers on aerosol optical depth, J. Geophys. Res. Atmos., 121, 336–361, https://doi.org/10.1002/2015JD023848, 2016.

Boney, S., and Dufresne, J. L.: Marine boundary layer clouds at the heart of tropical cloud feedback uncertainties in climate models, Geophys. Res. Lett., 32, L20806, https://doi.org/10.1029/2005GL023851, 2006.

Bréon, F.-M., Tanré, D., and Generoso, S.: Aerosol effect on cloud droplet size monitored from satellite, Science, 295(5556), 834–838, https://doi.org/10.1126/science.1066434, 2002.

Broekhuizen, K., Chang, R. Y. W., Leaitch, W. R., Li, S. M., and Abbatt, J. P. D.: Closure between measured and modeled cloud condensation nuclei (CCN) using size-resolved aerosol compositions in downtown Toronto, Atmos. Chem. Phys., 6, 2513–2524, https://doi.org/10.5194/acp-6-2513-2006, 2006.

Cecchini, M. A., Machado, L. A. T., Comstock, J. M., Mei, F., Wang, J., Fan, J., Tomlinson, J. M., Schmid, B., Albrecht, R., Martin, S. T., and Artaxo, P.: Impacts of the Manaus pollution

Deleted: -69

Deleted: -

Deleted: :

Deleted: -

Deleted: :

Deleted: :

Deleted: :

Deleted: -838

Deleted: sizeresolved

Deleted: -

plume on the microphysical properties of Amazonian warm-phase clouds in the wet season, Atmos. Chem. Phys., 16(11), 7029–7041, https://doi.org/10.5194/acp-16-7029-2016, 2016.

Chen, R., Li, Z., Kuligowski, R. J., Ferraro, R., and Weng, F.: A study of warm rain detection using A-Train satellite data, Geophys. Res. Lett., 38, L04804, https://doi.org/10.1029/2010GL046217, 2011.

Chiu, J. C., Huang, C. H., Marshak, A., Slutsker, I., Giles, D. M., Holben, B. N., Knyazikhin, Y., and Wiscombe, W. J.: Cloud optical depth retrievals from the Aerosol Robotic Network (AERONET) cloud mode observations, J. Geophys. Res. Atmos., 115, D14202, https://doi.org/10.1029/2009JD013121, 2010.

Clothiaux, E. E., Ackerman, T. P., Mace, G. G., Moran, K. P., Marchand, R. T., Miller, M. A., and Martner, B. E.: Objective determination of cloud heights and radar reflectivities using a combination of active remote sensors at the ARM CART sites, J. Appl. Meteor., 39, 645–665, https://doi.org/10.1175/1520-0450(2000)039<0645:ODOCHA>2.0.CO;2, 2000.

Crilley, L. R., Jayaratne, E. R., Ayoko, G. A., Miljevic, B., Ristovski, Z., and Morawska, L.: Observations on the formation, growth and chemical composition of aerosols in an urban environment, Environ. Sci. Technol., 48(12), 6588–6596, https://doi.org/10.1021/es5019509, 2014.

Dong, X., Minnis, P., Xi, B., Sun-Mack, S., and Chen, Y.: Comparison of CERES-MODIS stratus cloud properties with ground-based measurements at the DOE ARM Southern Great Plains site, J. Geophys. Res. Atmos., 113, D03204, https://doi.org/10.1029/2007JD008438, 2008.

Dusek, U., Frank, G. P., Hildebrandt, L., Curtius, J., Schneider, J., Walter, S., Chand, D., Drewnick, F., Hings, S., Jung, D., Borrmann, S., and Andreae, M. O.: Size matters more than chemistry for cloud-nucleating ability of aerosol particles, Science, 312 (5778), 1375–1378, https://doi.org/10.1126/science.1125261, 2006.

Eck, T. F., Holben, B. N., Reid, J. S., Dubovik, O., Smirnov, A., O'Neill, N. T., Slutsker, I. and Kinne, S.: Wavelength dependence of the optical depth of biomass burning, urban, and desert dust aerosols, J. Geophys. Res. Atmos., 104, https://doi.org/:10.1029/1999JD900923, 1999.

Feingold, G., Eberhard, W. L., Veron, D. E., and Previdi, M.: First measurements of the Twomey indirect effect using ground-based remote sensors, Geophys. Res. Lett., 30(6), 1827, https://doi.org/10.1029/2002GL016633, 2003.

Deleted: -
Deleted: :
Deleted: :
Deleted: :
Deleted: -
Deleted: -
Deleted: :
Deleted: :
Deleted: -1378
Deleted: :
Moved (insertion) [2]
Moved (insertion) [3]

Feingold, G., Furrer, R., Pilewskie, P., Remer, L. A., Min, Q., and Jonsson, H.: Aerosol indirect effect studies at Southern Great Plains during the May 2003 Intensive Operations Period, J. Geophys. Res. Atmos., 111, D05S14, https://doi.org/10.1029/2004JD005648, 2006.

Garrett, T. J., and Zhao, C.: Increased Arctic cloud longwave emissivity associated with pollution from mid-latitudes, Nature, 440, 787–789, https://doi.org/10.1038/nature04636, 2006.

Garrett, T. J., and Zhao, C.: Ground-based remote sensing of thin clouds in the Arctic, Atmos. Meas. Tech., 6, 1227–1243, https://doi.org/10.5194/amt-6-1227-2013, 2013.

Garrett, T. J., Zhao, C., Dong, X., Mace, G. G., and Hobbs, P. V.: Effects of varying aerosol regimes on low-level Arctic stratus, Geophys. Res. Lett., 31, L17105, https://doi.org/10.1029/2004GL019928, 2004.

Han, Q., Rossow, W. B., Zeng, J., and Welch, R.: Three different behaviors of liquid water path of water clouds in aerosol-cloud interactions, J. Atmos. Sci., 59, 726–735, https://doi.org/10.1175/1520-0469(2002)059<0726:TDBOLW>2.0.CO;2, 2002.

Hao, L., Romakkaniemi, S., Kortelaninen, A., Jaatinen, A., Portin, H., Miettinen, P., Komppula, M., Leskinen, A., Virtanen, A., Smith, J. N., Sueper, D., Worsnop, D. R., Lehtinen, K. E. J., and Laaksonen, A.: Aerosol chemical composition in cloud events by high resolution time-of-flight aerosol mass spectrometry, Environ. Sci. Technol., 47(6), 2645–2653, https://doi.org/10.1021/es302889w, 2013.

Harikishan, G., Padmakumari, B., Maheskumar, R. S., Pandithurai, G., and Min, Q. L.: Aerosol indirect effects from ground-based retrievals over the rain shadow region in Indian subcontinent, J. Geophys. Res. Atmos., 121, 2369–2382, https://doi.org/10.1002/2015JD024577, 2016.

Hill, A., Feingold, G., and Jiang, H.: The influence of entrainment and mixing assumption on aerosol–cloud interactions in marine stratocumulus, J. Atmos. Sci., 66, 1450–1464, https://doi.org/10.1175/2008JAS2909.1, 2009.

Holben, B. N., Kaufman, Y. J., and Eck, T. F.: AERONET: a federated instrument network and data archive for aerosol characterization, Remote Sens. Environ., 66, 1–16, https://doi.org/10.1016/S0034-4257(98)00031-5, 1998.

IPCC, Climate Change 2013: The Physical Science Basis. Contribution of Working Group I to the Fifth Assessment Report of the Intergovernmental Panel on Climate Change [Stocker, T. F., D. Qin, G.-K. Plattner, M. Tignor, S.K. Allen, J. Boschung, A. Nauels, Y. Xia, V. Bex, and

Deleted: :

Moved (insertion) [4]

Moved (insertion) [5]

Moved (insertion) [6]

Moved up [2]: Feingold, G., Eberhard, W. L., Veron, D. E., and Previdi, M.: First measurements of the Twomey indirect effect using ground-based remote sensors, Geophys. Res. Lett.,

Moved up [3]: Lett., 30(6), 1827,

Deleted: doi:10.1029/2002GL016633, 2003.¶

Deleted: -

Deleted: -

Deleted: :

Deleted: :

Deleted: -16

Deleted: (2013),

P. M. Midgley (eds.)]. Cambridge University Press, Cambridge, United Kingdom and New York, NY, USA, 1535 pp, https://doi.org/10.1017/CBO9781107415324, 2013.

Jefferson, A.: Aerosol observing system (AOS) handbook, ARMTR-014, U.S. Dep. of Energy, Washington, D. C., 2011.

Johnson, B. T., Shine, K. P., and Forster, P. M.: The semi-direct aerosol effect: Impact of absorbing aerosols on marine stratocumulus, Q. J. R. Meteorol. Soc., 130(599), 1407–1422, https://doi.org/10.1256/qj.03.61, 2004.

Kaufman, Y. J., Koren, I., Remer, L. A., Rosenfeld, D., and Rudich, Y.: The effect of smoke, dust, and pollution aerosol on shallow cloud development over the Atlantic Ocean, Proc. Natl. Acad. Sci., 102(32), 11,207–11,212, https://doi.org/10.1073/pnas.0505191102, 2005.

Kim, B.-G., Schwartz, S. E., Miller, M. A., and Min, Q.: Effective radius of cloud droplets by ground-based remote sensing: relationship to aerosol, J. Geophys. Res. Atmos., 108(D23), 4740, https://doi.org/10.1029/2003JD003721, 2003.

Kim, B.-G., Miller, M. A., Schwartz, S. E., Liu, Y., and Min, Q.: The role of adiabaticity in the aerosol first indirect effect, J. Geophys. Res. Atmos., 113(D5), https://doi.org/10.1029/2007JD008961, 2008.

Kollias, P., Clothiaux, E. E., Miller, M. A., Luke, E. P., Johnson, K. L., Moran, K. P., Widener, K. B., and Albrecht, B. A.: The Atmospheric Radiation Measurement Program cloud profiling radars: second-generation sampling strategies, processing, and cloud data products, J. Atmos. Oceanic Technol., 24, 1199–1214, https://doi.org/10.1175/JTECH2033.1, 2007.

Komppula, M., Lihavainen, H., Kerminen, V.-M., Kulmala, M., and Viisanen, Y.: Measurements of cloud droplet activation of aerosol particles at a clean subarctic background site, J. Geophys. Res. Atmos., 110, D06204, https://doi.org/10.1029/2004JD005200, 2005.

Koren, I., Kaufman, Y. J., Remer, L. A., and Martins, J. V.: Measurement of the effect of Amazon smoke on inhibition of cloud formation, Science, 303, 1342–1345, https://doi.org/10.1126/science.1089424, 2004.

Lebsock, M. D., Stephens, G. L., and Kummerow, C.: Multisensor satellite observations of aerosol effects on warm clouds, J. Geophys. Res. Atmos., 113, D15205, https://doi.org/10.1029/2008JD009876, 2008.

Deleted: :

Deleted: -

Deleted: :

Deleted: 11207-11212

Deleted: :

Moved (insertion) [7]

Moved (insertion) [8]

Moved (insertion) [9]

Deleted: :

Deleted: :

Li, Z., Niu, F., Fan, J., Liu, Y., Rosenfeld, D., and Ding, Y.: Long-term impacts of aerosols on the vertical development of clouds and precipitation, Nature Geosci., 4(12), 888–894, https://doi.org/10.1038/ngeo1313, 2011.

Li, Z., Rosenfeld, D., and Fan, F.: Aerosols and their impact on radiation, clouds, precipitation, and severe weather events, *Oxford Research Encyclopedias*, doi:10.1093/acrefore/9780199389414.013.126, 2017.

Li, Z., et al.: Aerosol and monsoon interactions in Asia, *Rev. Geophys*., 10.1002/2015 RG000500, 2016.

Lihavainen, H., Kerminen, V. M., and Remer, L. A.: Aerosol-cloud interaction determined by both in situ and satellite data over a northern high-latitude site, Atmos. Chem. Phys., 10(22), 10,987–10,995, https://doi.org/10.5194/acp-10-10987-2010, 2010.

Liljegren J. C., and Lesht, B. M.: Preliminary results with the twelve-channel microwave radiometer profiler at the North Slope of Alaska Climate Research Facility, Fourteenth ARM Science Team Meeting Proceedings, Albuquerque, New Mexico, 2004.

Liu, J., and Li, Z.: Estimation of cloud condensation nuclei concentration from aerosol optical quantities: influential factors and uncertainties, Atmos. Chem. Phys., 14(1), 471–483, https://doi.org/10.5194/acp-14-471-2014, 2014.

Liu, J., and Li, Z.: First surface-based estimation of the aerosol indirect effect over a site in southeastern China, Adv. Atmos. Sci., 35(2), 169–181, https://doi.org/10.1007/s00376-017-7106-2, 2018a.

Liu, J., and Li, Z.: Significant underestimation in the optically-based estimation of the aerosol first indirect effect induced by the aerosol swelling effect, Geophys. Res. Lett., 45(11), https://doi.org/10.1029/2018GL077679, 2018b.

Liu, J., Zheng, Y., Li, Z., and Cribb, M.: Analysis of cloud condensation nuclei properties at a polluted site in southeastern China during the AMF-China Campaign, J. Geophys. Res. Atmos., 116, D00K35, https://doi.org/10.1029/2011jd016395, 2011.

Liu, J., Zheng, Y., Li, Z., Flynn, C., and Cribb, M.: Seasonal variations of aerosol optical properties, vertical distribution and associated radiative effects in the Yangtze Delta region of China, J. Geophys. Res., 117, D00K38, https://doi.org/10.1029/2011JD016490, 2012.

Liu, J., Li, Z., Zheng, Y., Chiu, J. C., Zhao, F., Cadeddu, M., Weng, F., and Cribb, M.: Cloud optical and microphysical properties derived from ground-based and satellite sensors over a

Deleted: -

Deleted: :http://www.nature.com/ngeo/journal/v4/n12/abs

Deleted: 10987-10995,

Deleted: :

Deleted: .

Moved (insertion) [10]

Moved (insertion) [11]

Moved (insertion) [12]

Moved (insertion) [13]

Moved (insertion) [14]

Deleted: :

Moved up [10]: Liu, J., and Li, Z.: Estimation of cloud condensation nuclei concentration from aerosol optical quantities: influential factors and uncertainties, Atmos. Chem. Phys., 14(1), 471-483, doi:10.5194/acp-14-471-2014

Moved up [11]: Phys., 14(1), 471

Deleted: -483, doi:10.5194/acp-14-471-2014, 2014.¶

Moved up [12]: Liu, J., and Li, Z.: First surface-based estimation of the aerosol indirect effect over a site in southeastern China, Adv. Atmos. Sci.,

Moved up [13]: Sci., 35(2), 169

Deleted: -181, 2018a.¶

Moved up [14]: Liu, J., and Li, Z.: Significant underestimation in the optically-based estimation of the aerosol first indirect effect induced by the aerosol swelling effect, Geophys. Res. Lett.,

Deleted: https://doi.org/10.1029/2018GL077679, 2018b.¶

site in the Yangtze Delta region, J. Geophys. Res. Atmos., 118, https://doi.org/10.1002/jgrd.50648, 2013.

Liu, J., Li, Z., and Cribb, M.: Response of marine boundary layer cloud properties to aerosol perturbations associated with meteorological conditions from the 19-month AMF-Azores campaign, J. Atmos. Sci., 73(11), 4253–4268, https://doi.org/10.1175/JAS-D-15-0364.1, 2016.

Lohmann, U., Rotstayn, L., Storelvmo, T., Jones, A., Menon, S., Quaas, J., Ekman, A. M. L., Koch, D., and Ruedy, R.: Total aerosol effect: radiative forcing or radiative flux perturbation?, Atmos. Chem. Phys., 10, 3235–3246, https://doi.org/10.5194/acp-10-3235-2010, 2010.

Matsui, T., Masunaga, H., Pielke Sr., R. A., and Tao, W.-K.: Impact of aerosols and atmospheric thermodynamics on cloud properties within the climate system, Geophys. Res. Lett., 31, L06109, https://doi.org/10.1029/2003GL019287, 2004.

McComiskey, A., and Feingold, G.: Quantifying error in the radiative forcing of the first aerosol indirect effect, Geophys. Res. Lett., 35(2), L02810, https://doi.org/10.1029/2007GL032667, 2008.

McComiskey, A., Feingold, G., Frisch, A. S., Turner, D. D., Miller, M. A., Chiu, J. C., Min, Q., and Ogren, J. A.: An assessment of aerosol-cloud interactions in marine stratus clouds based on surface remote sensing, J. Geophys. Res. Atmos., 114, D09203, https://doi.org/10.1029/2008JD011006, 2009.

McFiggans, G., Artaxo, P., Baltensperger, U., Coe, H., Facchini, M., Feingold, G., Fuzzi, S., Gysel, M., Laaksonen, A., Lohmann, U., Mentel, T., Murphy, D., O'Dowd, C. D., Snider, J. R., and Weingartner, E.: The effect of physical and chemical aerosol properties on warm cloud droplet activation, Atmos. Chem. Phys., 6, 2593–2649, https://doi.org/10.5194/acp-6-2593-2006, 2006.

Medeiros, B., and Stevens, B.: Revealing differences in GCM representations of low clouds, Clim. Dyn., 36, 385–399, https://doi.org/10.1007/s00382-009-0694-5, 2011.

Ng, N. L., Herndon, S. C., Trimborn, A., Canagaratna, M., Croteau, P., Onasch, T. B., Sueper, D., Worsnop, D. R., Zhang, Q., Sun, Y. L., and Jayne, J. T.: An Aerosol Chemical Speciation Monitor (ACSM) for routine monitoring of the composition and mass concentrations of ambient aerosol, Aerosol Sci. Technol., 45(7), 770–784, https://doi.org/10.1080/02786826.2011.560211, 2011.

Deleted: :

Deleted: -

Deleted: :

Deleted: -

Deleted: :

Deleted: :

Deleted: :

Deleted: -

Deleted: -399

Deleted: Menon, S., Del Genio, A. D., Koch, D., and Tseloudis, G.: GCM simulations of the aerosol indirect effect: sensitivity to cloud parameterization and aerosol burden, J. Atmos. Sci., 59, 692-713, 2002.¶
Nakajima, T., Higurashi,

Moved up [7]: A.,

Deleted: Kawamoto, K., and Penner, J. E.: A possible correlation between satellite-derived cloud and aerosol microphysical parameters, Geophys.

Moved up [6]: Res. Lett.,

Deleted: 28(7), 1171-1174, 2001.¶

Deleted:):

Deleted: -

Painemal, D., and Zuidema, P.: The first aerosol indirect effect quantified through airborne remote sensing during VOCALS-REx, Atmos. Chem. Phys., 13(2), 917–931, https://doi.org/10.5194/acp-13-917-2013, 2013.

Pandithurai, G., Takamura, T., Yamaguchi, J., Miyagi, K., Takano, T., Ishizaka, Y., Dipu, S., and Shimizu, A.: Aerosol effect on cloud droplet size as monitored from surface-based remote sensing over East China Sea region, Geophys. Res. Lett., 36, L13805, https://doi.org/10.1029/2009GL038451, 2009.

Portin, H., Leskinen, A., Hao, L., Kortelainen, A., Miettinen, P., Jaatinen, A., Laaksonen, A., Lehtinen, K. E. J., Romakkaniemi, S., and Komppula, M.: The effect of local sources on particle size and chemical composition and their role in aerosol–cloud interactions at Puijo measurement station, Atmos. Chem. Phys., 14, 6021–6034, https://doi.org/10.5194/acp-14-6021-2014, 2014.

Qiu, Y., Zhao, C., Guo, J., and Li, J.: Eight-year ground-based observational analysis about the seasonal variation of the aerosol-cloud droplet effective radius relationship at SGP site, Atmos. Environ., 164, 139–146, https://doi.org/10.1016/j.atmosenv.2017.06.002, 2017.

Raymond, T. M., and Pandis, S. N.: Formation of cloud droplets by multicomponent organic particles, J. Geophys. Res. Atmos., 108, 4469, https://doi.org/10.1029/2003JD003503, 2002.

Rolph, G. D.: Real-time Environmental Applications and Display sYstem (READY) Website (http://www.ready.noaa.gov), NOAA Air Resources Laboratory, College Park, MD, 2016.

Sekiguchi, M., Nakajima, T., Suzuki, K., Kawamoto, K., Higurashi, A., Rosenfeld, D., Sano, I., and Mukai, S.: A study of the direct and indirect effects of aerosols using global satellite data sets of aerosol and cloud parameters, J. Geophys. Res. Atmos., 108, 4699, https://doi.org/10.1029/2002JD003359, D22, 2003.

Sena, E. T., McComiskey, A., and Feingold, G.: A long-term study of aerosol-cloud interactions and their radiative effect at the Southern Great Plains using ground-based measurements, Atmos. Chem. Phys., 16, 11,301–11,318, https://doi.org/10.5194/acp-16- 11301-2016, 2016.

Sporre, M. K., Glantz, P., Tunved, P., Swietlicki, E., Kulmala, M., and Lihavainen, H.: A study of the indirect aerosol effect on subarctic marine liquid low-level clouds using MODIS cloud data and ground-based aerosol measurements, Atmos. Res., 116(0), 56–66, https://doi.org/10.1016/j.atmosres.2011.09.014, 2012.

Moved (insertion) [15]

Moved (insertion) [16]

Deleted: :

Moved up [15]: Painemal, D., and Zuidema, P.: The first aerosol indirect effect quantified through airborne remote sensing during VOCALS-REx, Atmos. Chem. Phys., 13(2), 917

Moved up [16]: Phys., 13(2), 917

Deleted: -931, doi:10.5194/acp-13-917-2013, 2013.¶

Moved up [8]: Kollias, P., Clothiaux, E. E., Miller, M. A., Luke, E. P., Johnson, K. L., Moran, K. P., Widener, K. B., and Albrecht, B. A.: The Atmospheric Radiation Measurement Program cloud profiling radars: second-generation sampling strategies, processing, and cloud data products, J. Atmos. Oceanic

Moved up [9]: Oceanic Technol., 24, 1199–1214,

Deleted: doi:10.1175/JTECH2033.1, 2007.¶

Deleted: :

Deleted: 2002.

Deleted: :

Moved (insertion) [17]

Moved down [18]: Sporre, M. K., Swietlicki, E., Glantz, P., and Kulmala, M.: Aerosol indirect effects on continental low-level clouds over Sweden and Finland, Atmos. Chem. Phys., 14(22),

Moved down [19]: Phys., 14(22),

Deleted: 12167-12179, doi:10.5194/acp-14-12167-2014, 2014.¶

Deleted: -

Deleted: doi:http://dx.

Sporre, M. K., Swietlicki, E., Glantz, P., and Kulmala, M.: Aerosol indirect effects on continental low-level clouds over Sweden and Finland, Atmos. Chem. Phys., 14(22), 12,167–12,179, https://doi.org/10.5194/acp-14-12167-2014, 2014.

Stein, A. F., Draxler, R. R, Rolph, G. D., Stunder, B. J. B., Cohen, M. D., and Ngan, F.: NOAA's HYSPLIT atmospheric transport and dispersion modeling system, Bull. Amer. Meteor. Soc., 96, 2059–2077, https://doi.org/10.1175/BAMS-D-14-00110.1, 2015.

Su, W., Loeb, N. G., Xu, K.-M., Schuster, G. L., and Eitzen, Z. A.: An estimate of aerosol indirect effect from satellite measurements with concurrent meteorological analysis, J. Geophys. Res. Atmos., 115(D18), D18219, https://doi.org/10.1029/2010jd013948, 2010.

Twohy, C. H., Anderson, J. R., Toohey, D. W., Andrejczuk, M., Adams, A., Lytle, M., George, R. C., Wood, R., Saide, P., Spak, S., Zuidema, P., and Leon, P.: Impacts of aerosol particles on the microphysical and radiative properties of stratocumulus clouds over the southeast Pacific Ocean, Atmos. Chem. Phys., 13(5), 2541–2562, https://doi.org/10.5194/acp-13-2541-2013, 2013.

Twomey, S.: The influence of pollution on the shortwave albedo of clouds, J. Atmos. Sci., 34, 1149–1152, https://doi.org/10.1175/1520-0469(1977)034<1149:TIOPOT>2.0.CO;2, 1977.

Wang, F., Guo, J., Wu, Y., Zheng, X., Deng, M., Li, X., Zhang, J., and Zhao, J.: Satellite observed aerosol-induced variability in warm cloud properties under different meteorological conditions over eastern China, Atmos. Environ., 84, 122–132, https://doi.org/10.1016/j.atmosenv.2013.11.018, 2014.

Wang, J., Flagan, R. C., and Seinfeld, J. H.: A differential mobility analyzer (DMA) system for submicron aerosol measurements at ambient relative humidity, Aerosol Sci. Technol., 37, 46–52, https://doi.org/10.1080/02786820300891, 2003.

Wang, J., Lee, Y.-N., Daum, P. H., Jayneand, J., and Alexander, M. L.: Effects of aerosol organics on cloud condensation nucleus (CCN) concentration and first indirect aerosol effect, Atmos. Chem. Phys., 8, 6325–6339, https://doi.org/10.5194/acp-8-6325-2008, 2008.

Werner, F., Ditas, F., Siebert, H., Simmel, M., Wehner, B., Pilewskie, P., Schmeissner, T., Shaw, R. A., Hartmann, S., Wex, H., Roberts, G. C., and Wendisch, M.: Twomey effect observed from collocated microphysical and remote sensing measurements over shallow cumulus, J. Geophys. Res. Atmos., 119, https://doi.org/10.1002/2013JD020131, 2014.

Moved (insertion) [18]

Moved (insertion) [19]

Deleted: -

Deleted: http://dx.

Deleted: :

Deleted: Titos,

Moved up [5]: G.,

Deleted: Jefferson, A., Sheridan, P.

Moved up [4]: J.,

Deleted: Andrews, E., Lyamani, H., Alados-Arboledas, L., and Ogren, J. A.: Aerosol light-scattering enhancement due to water uptake during the TCAP campaign, Atmos.

Moved up [17]: Chem.

Deleted: Phys., 14(13), 7031-7043, doi:10.5194/acp-14-7031-2014, 2014.¶

Deleted: -

Deleted: :

Deleted: 1977.

Deleted: -

Deleted: -52

Deleted: -

Deleted: :

Deleted: :

West, R. E. L., Stier, P., Jones, A., Johnson, C. E., Mann, G. W., Bellouin, N., Partridge, D. G., and Kipling, Z.: The importance of vertical velocity variability for estimates of the indirect aerosol effects, Atmos. Chem. Phys., 14(12), 6369–6393, https://doi.org/10.5194/acp-14-6369-2014, 2014.

Yan, H., Li, Z., Huang, J., Cribb, M., and Liu, J.: Long-term aerosol-mediated changes in cloud radiative forcing of deep clouds at the top and bottom of the atmosphere over the Southern Great Plains, Atmos. Chem. Phys., 14(14), 7113–7124, https://doi.org/10.5194/acp-14-7113-2014, 2014.

Yang, X., Zhao, C. F., Zhou, L. J., Wang, Y., and Liu, X. H.: Distinct impact of different types of aerosols on surface solar radiation in China, J. Geophys. Res. Atmos., 121, 6459–6471, https://doi.org/10.1002/2016JD024938, 2016.

Yang, X., Zhao, C., Zhou, L., Li, Z., Cribb, M., and Yang, S.: Wintertime cooling and a potential connection with transported aerosols in Hong Kong during recent decades, Atmos. Res., 211, 52–61, https://doi.org/10.1016/j.atmosres.2018.04.029, 2018.

Yang, Y., Zhao, C., Dong, X., Fan, G., Zhou, Y., Wang, Y., Zhao, L., Lv, F. and Yan, F.: Toward understanding the process-level impacts of aerosols on microphysical properties of shallow cumulus cloud using aircraft observations, Atmos. Res., 221, 27–33, https://doi.org/10.1016/j.atmosres.2019.01.027, 2019.

Zhang, Q., Quan, J., Tie, X., Huang, M., and Ma, X.: Impact of aerosol particles on cloud formation: aircraft measurements in China, Atmos. Environ., 45(3), 665–672, https://doi.org/10.1016/j.atmosenv.2010.10.025, 2011.

Zhao, C., and Garrett, T.: Effects of Arctic haze on surface cloud radiative forcing, Geophys. Res. Lett., 42, 557–564, https://doi.org/10.1002/2014GL062015, 2015.

Zhao, C., et al.: Toward understanding of differences in current cloud retrievals of ARM ground-based measurements, J. Geophys. Res. Atmos., 117, D10206, https://doi.org/10.1029/2011JD016792, 2012a.

Zhao, C., Klein, S. A., Xie, S., Liu, X., Boyle, J. S., and Zhang, Y.: Aerosol first indirect effects on non-precipitating low-level liquid cloud properties as simulated by CAM5 at ARM sites, Geophys. Res. Lett., 39(8), L08806, https://doi.org/10.1029/2012gl051213, 2012b.

Deleted: -
Deleted: :
Deleted: -
Deleted: :
Deleted: Yuan, T., Li, Z., Zhang, R
Deleted: Fan, J.: Increase
Deleted: cloud droplet size with aerosol optical depth: An observation and modeling study
Deleted: 113, D04201,
Deleted: :
Deleted: 1029/2007JD008632, 2008
Deleted: -
Deleted: doi:http://dx.
Deleted: :
Deleted: 2012

Zhao, C., Qiu, Y., Dong, X., Wang, Z., Peng, Y., Li, B., Wu, Z., and Wang, Y.: Negative aerosol-cloud r_e relationship from aircraft observations over Hebei, China, Earth and Space Science, 5, 19–29, https://doi.org/10.1002/2017EA000346, 2018.

Zhao, C., Zhao, L., and Dong, X.: A case study of stratus cloud properties using in situ aircraft observations over Huanghua, China, Atmosphere, 10(1), 19, https://doi.org/10.3390/atmos10010019, 2019.

Table 1. Seasonally averaged aerosol properties during the campaign period.

Deleted: Seasonal mean of

	Spring	Summer	Autumn	Winter	Annual
σ_1 (Mm^{-1})	14.2±14.1	33.7±28.0	14.4±13.6	12.8±11.7	18.1±19.3
σ_{10} (Mm^{-1})	31.2±25.3	45.0±32.9	26.5±20.4	26.3±23.6	31.7±26.7
σ_1 / σ_{10}	0.455	0.749	0.543	0.487	0.568
N_a (m^{-3})	2868±2367	2498±1536	2280±1854	2611±2108	2559±2014
SSA	0.95±0.04	0.96±0.03	0.95±0.04	0.94±0.04	0.95±0.04
AOD_{440}	0.11±0.08	0.19±0.14	0.11±0.11	0.08±0.05	0.13±0.1
AE	1.27±0.40	1.65±0.31	1.51±0.36	1.35±0.45	1.44±0.40

Deleted: Yearly

σ_1: scattering coefficient, fine-mode particles; σ_{10}: scattering coefficient, total; N_a: aerosol number concentration; SSA: single-scattering albedo; AOD_{440}: aerosol optical depth at 440 nm; AE: Ångström exponent

Deleted: Angstrom

Table 2. Means and standard deviations of aerosol and cloud properties for each air-mass cluster.

Air Mass	σ_1 (Mm^{-1})	σ_{10} (Mm^{-1})	σ_1/σ_{10}	N_a (m^{-3})	SSA	AOD_{440}	AE	COD	LWP ($g\ m^{-2}$)	DER (µm)
I	19.8±21.4	30.6±26.8	0.65	2969±2183	0.94±0.04	0.13±0.12	1.6±0.4	25.7±14.5	127±99	7.9±4.8
II	14.5±14.6	30.8±25.6	0.47	1788±1322	0.96±0.04	0.11±0.08	1.3±0.5	33.0±18.3	243±197	10.9±6.6
III	16.4±15.6	34.5±27.2	0.48	1937±1558	0.96±0.03	0.12±0.06	1.3±0.4	26.4±16.5	162±121	9.8±4.9

σ_1: scattering coefficient, fine-mode particles; σ_{10}: scattering coefficient, total; N_a: aerosol number concentration; SSA: single-scattering albedo;
AOD_{440}: aerosol optical depth at 440 nm; AE: Ångström exponent;
COD: cloud optical depth; LWP: liquid water path; DER: cloud droplet effective radius

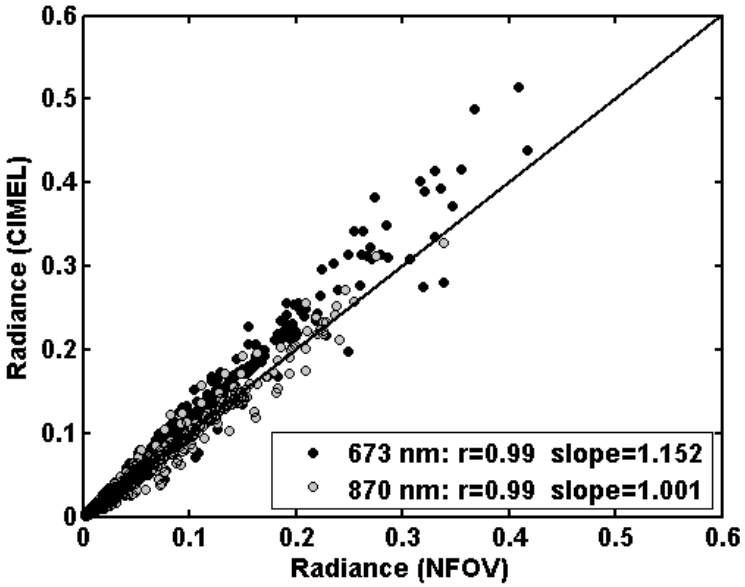

Figure 1. CIMEL sunphotometer-measured radiance as a function of narrow-field-of-view (NFOV) radiometer-measured radiance at 673 nm (black dots) and 870 nm (gray dots). The diagonal line represents the 1:1 line. Units are W sr^{-1} m^{-2}. The legend gives the coefficient of correlation (r) and the slope of the best-fit linear regression line through each dataset.

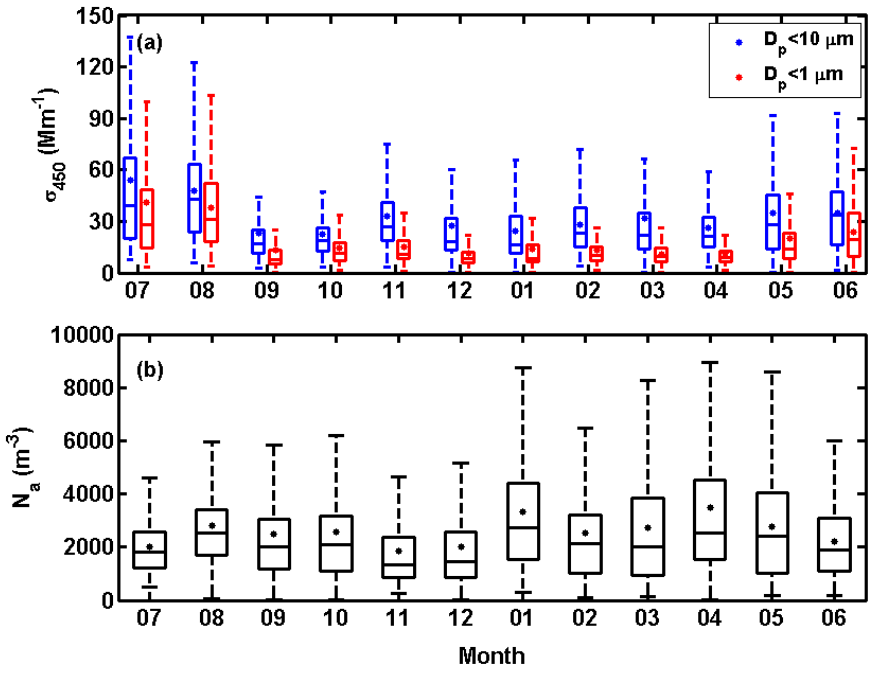

Figure 2. Monthly variations in (a) aerosol scattering coefficient at 450 nm (σ_{450}) for total (in blue, particle diameter, D_p, less than 10 μm) and fine-mode (in red, D_p less than 1 μm) aerosol particles and (b) aerosol particle number concentration (N_a). Box and whisker plots include median values (horizontal lines inside boxes), 25th and 75th percentiles (ends of boxes), 5th and 95th percentiles (ends of whiskers), and mean values (black dots). Months from left to right start at July 2012 and end at June 2013.

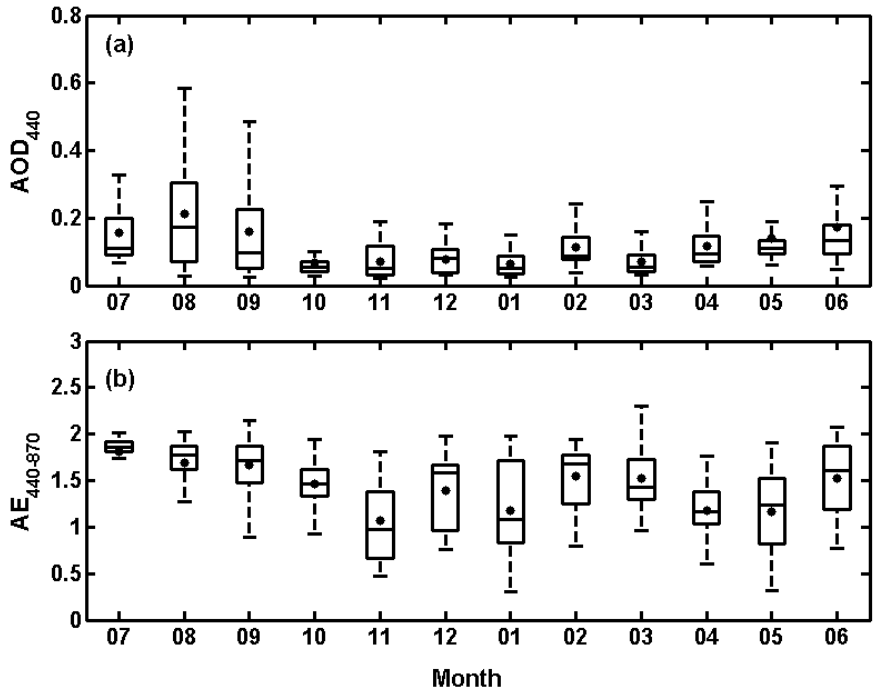

Figure 3. Monthly variations in columnar (a) aerosol optical depth at 440 nm (AOD_{440}) and (b) Ångström exponent (AE). Box and whisker plots include median values (horizontal lines inside boxes), 25th and 75th percentiles (ends of boxes), 5th and 95th percentiles (ends of whiskers), and mean values (black dots). Months from left to right start at July 2012 and end at June 2013.

Deleted: Angstrom

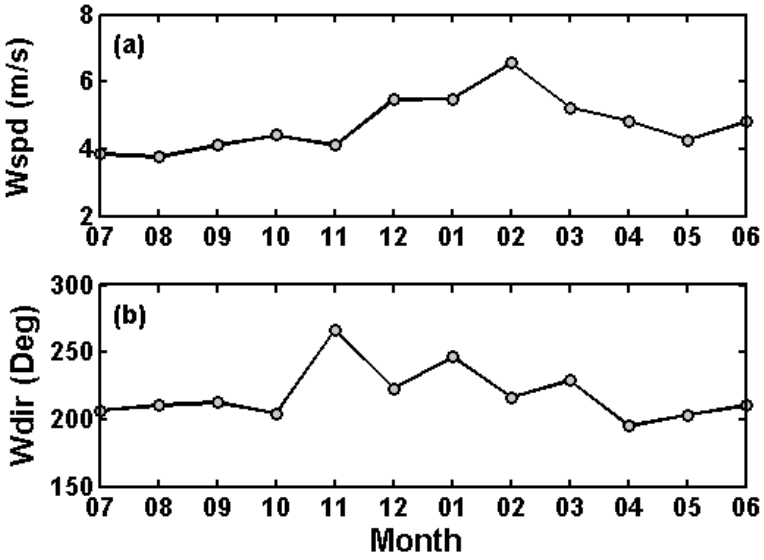

Figure 4. Monthly mean (a) wind speed (Wspd) and (b) wind direction (Wdir) during the campaign period. Months from left to right start at July 2012 and end at June 2013.

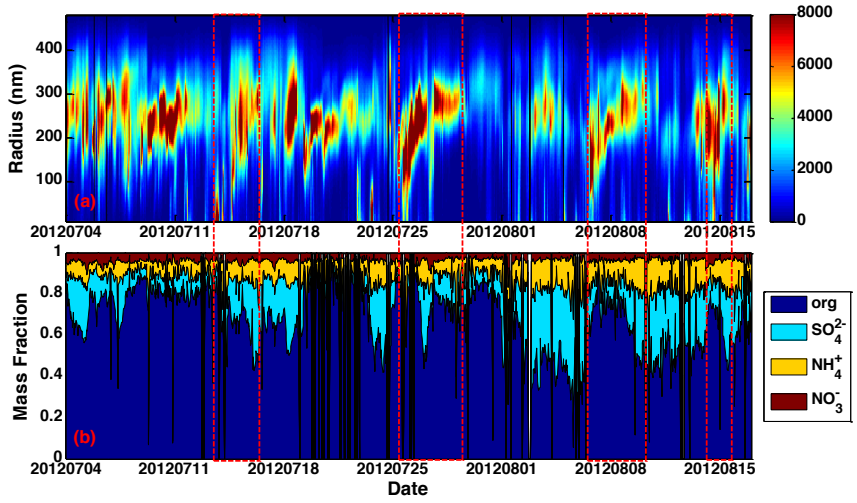

Figure 5. Time series of (a) particle size distribution and (b) mass fractions of organics (org, dark blue), sulfate (SO_4^{2-}, cyan), ammonium (NH_4^+, yellow), and nitrate (NO_3^-, red) in aerosols sampled during July and August of 2012. Dashed red rectangles outline periods of new particle formation and growth.

Deleted: fraction

Deleted: aqua

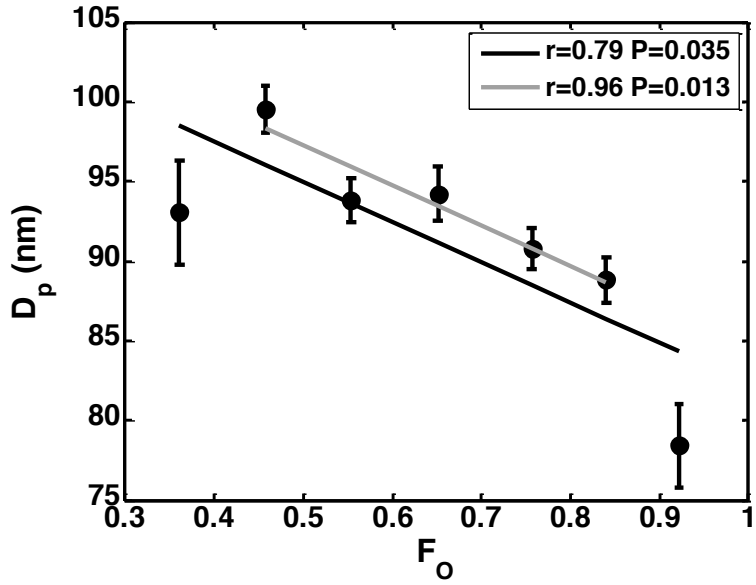

Figure 6. Mean aerosol particle radius (D_p) as a function of organic mass fraction (F_O). The black line is the linear regression line through all FO bins. The gray line is the linear regression line for F_O bins ranging from 0.4 to 0.9, which have the most samples. Data are from July and August of 2012. The legend gives the coefficient of correlation (r) and the statistical probability (P).

Deleted: for

Deleted: ¶

Page Break

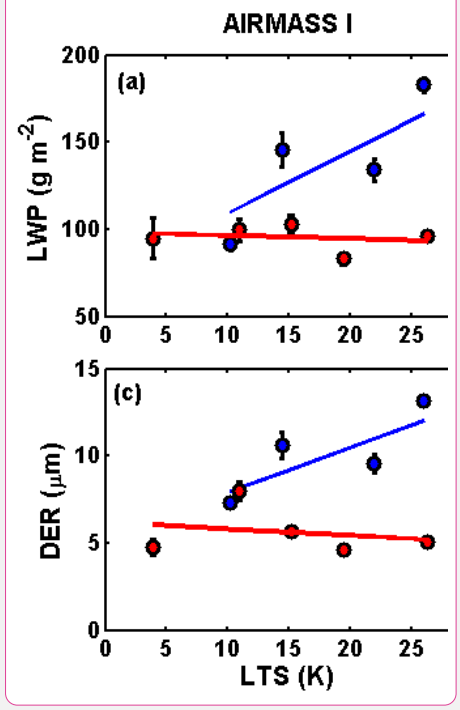

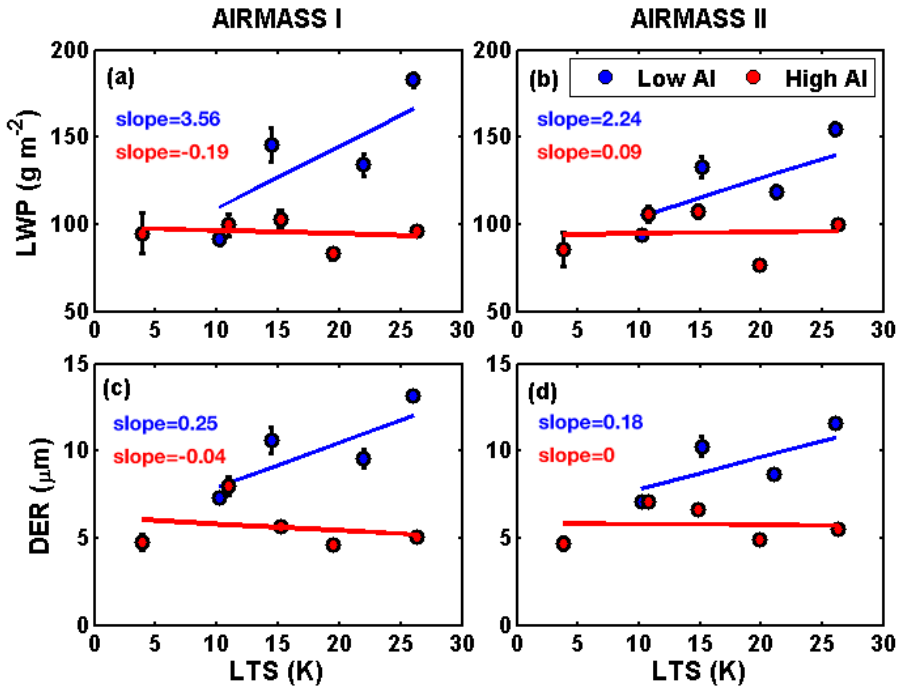

Figure 7. Liquid water path (LWP) and cloud droplet effective radius (DER) as functions of lower tropospheric stability (LTS) at low (in blue) and high (in red) scattering aerosol index (AI) levels under cluster I air-mass (a, c) and cluster II air-mass (b, d) conditions. Low and high scattering AI are defined as the lowest and highest quarter of all scattering AI samples, respectively.

Deleted: for

Deleted: , respectively.

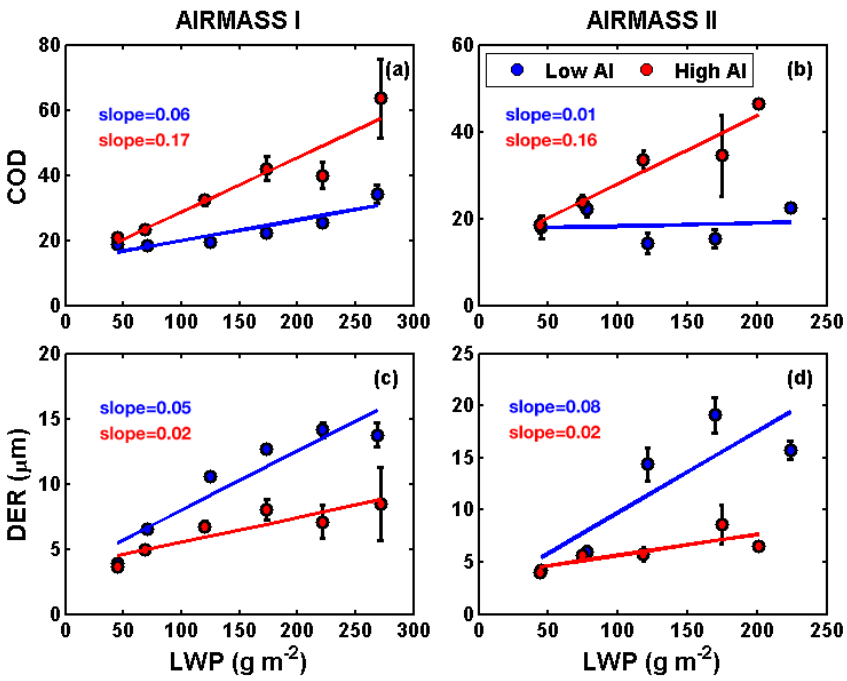

Figure 8. Cloud optical depth (COD) and cloud droplet effective radius (DER) as a function of liquid water path (LWP) at low (in blue) and high (in red) scattering aerosol index (AI) levels under cluster I air-mass (a, c) and cluster II air-mass (b, d) conditions. Low and high scattering AI are defined as the lowest and highest quarter of all scattering AI samples, respectively.

Deleted: ¶

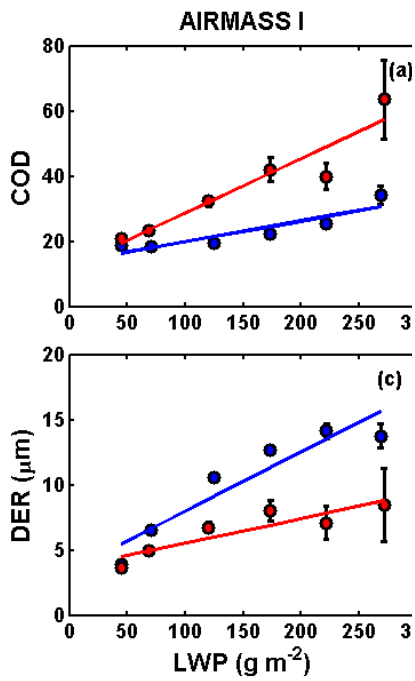

Deleted: for

Deleted: , respectively.

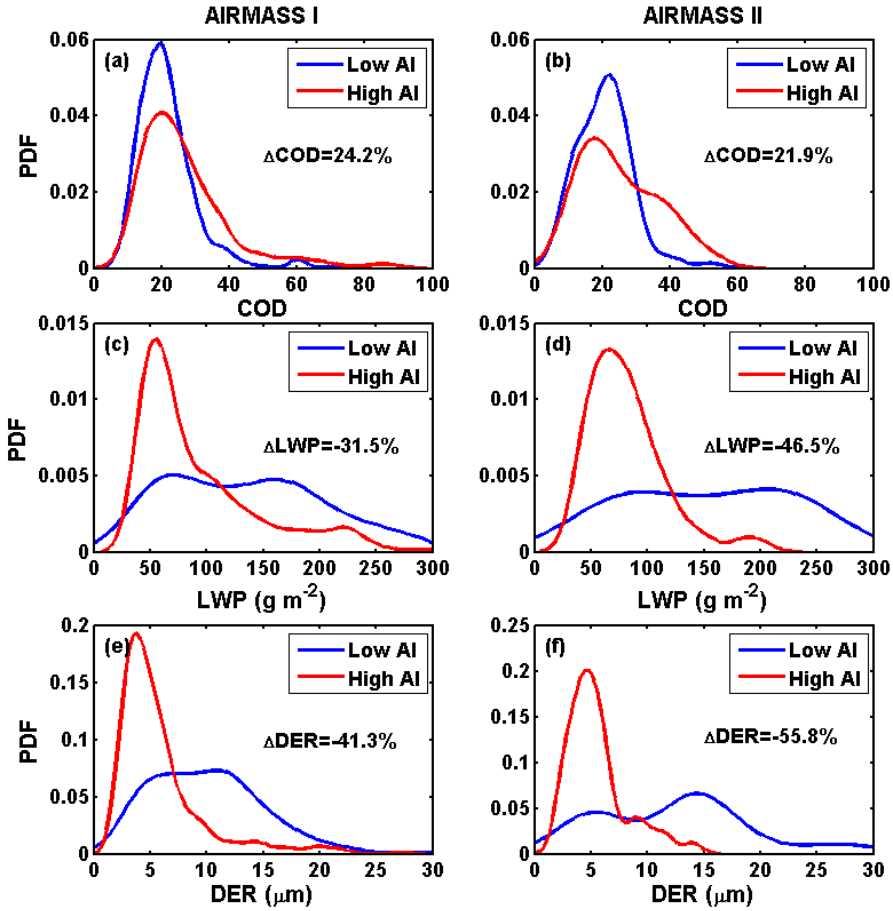

Figure 9. From top to bottom, probability distribution functions (PDFs) of cloud optical depth (COD), liquid water path (LWP), and cloud droplet effective radius (DER) at low (L, in blue) and high (H, in red) scattering aerosol index (AI) levels for the cluster I air mass (a, c, e) and the cluster II air mass (b, d, f). The mean percentage difference in COD, LWP and DER between high and low scattering AI levels {calculated as [(H – L / L)]*100%} is given in each panel.

Deleted: PDF

Deleted: -

Deleted: -

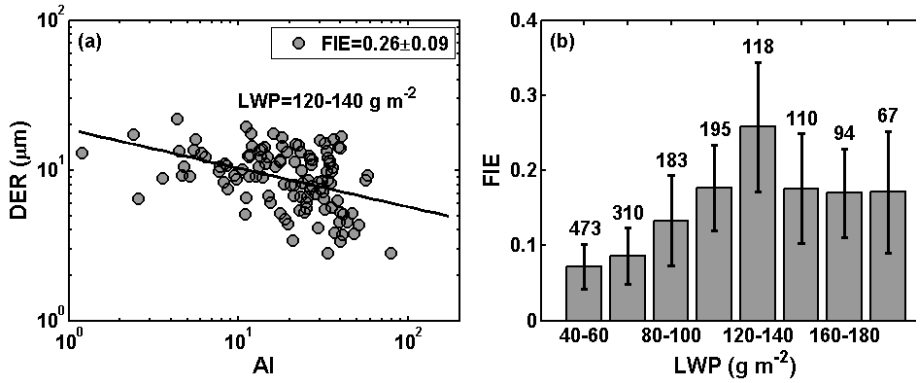

Figure 10. (a) Cloud droplet effective radius (DER) as a function of scattering aerosol index (AI) for a sample bin with a constant liquid water path (LWP) range of 120 to 140 g m^{-2}, and (b) the quantified aerosol first indirect effect (FIE) for each LWP bin. Numbers above each bar in (b) are the number of samples that went into the calculation of the FIE.

Deleted: equal

Deleted: 120-

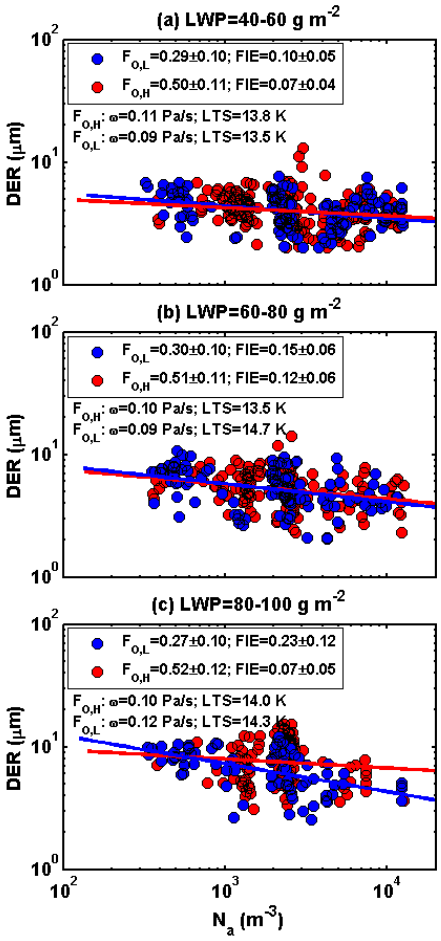

Figure 11. Cloud droplet effective radius (DER) as a function of aerosol number concentration (N_a) at low (in blue) and high (in red) levels of mass fraction of organics in three liquid water path (LWP) bins: (a) 40–60 g m^{-2}, (b) 60–80 g m^{-2}, and (c) 80–100 g m^{-2}. Linear regression lines through each set of data are drawn. $F_{o,l}$ and $F_{o,h}$ are defined as the means of values less than and greater than, respectively, the mean value of the mass fraction of organics from all samples in each LWP bin. The legend gives the mean values of $F_{o,l}$ and $F_{o,h}$ with their standard deviations and the magnitudes of the FIE with their uncertainties. Mean values of vertical velocity (ω) and lower tropospheric stability (LTS) corresponding to $F_{o,l}$ and $F_{o,h}$ levels in each LWP bin are also given.

Deleted: -
Deleted: -
Deleted: -
Deleted: Mean value
Deleted: magnitude
Deleted: are given in the legends.
Deleted: value
Deleted:),
Deleted: at
Deleted: shown.¶